

000 001 002 003 004 005 006 007 008 009 010 EFFECTIVENESS OF LOCAL STEPS ON HETEROGENEOUS DATA: AN IMPLICIT BIAS VIEW

005 **Anonymous authors**

006 Paper under double-blind review

ABSTRACT

011 In distributed training of machine learning models, gradient descent with *local iterative*
 012 *steps* is a very popular method to mitigate communication burden, commonly known
 013 as Local (Stochastic) Gradient Descent (Local-(S)GD). In the interpolation regime,
 014 Local-GD can converge to zero training loss. However, with many potential solutions
 015 corresponding to zero training loss, it is not known which solution Local-GD converges
 016 to. In this work we answer this question by analyzing implicit bias of Local-GD for
 017 classification tasks with *linearly separable data*. In the case of highly heterogeneous
 018 data, it has been observed empirically that local models can diverge significantly from
 019 each other (also known as “client drift”). However, for the interpolation regime, our
 020 analysis shows that the aggregated global model resultant from Local-GD with *arbitrary*
 021 *number* of local steps converges exactly to the model that would result in if all data
 022 were in one place (centralized trained model) in direction. Our result gives the exact
 023 rate of convergence to the centralized model with respect to the number of local steps.
 024 **We also obtain this same implicit bias with a learning rate independent of number of**
 025 **local steps with a Modified Local-GD algorithm for the case local problems are exactly**
 026 **solved.** Our analysis provides a new view to understand why Local-GD can still work
 027 very well with a very large number of local steps even for heterogeneous data. Lastly
 028 we also discuss the extension of our results to Local SGD and non-separable data.

029 1 INTRODUCTION

030
 031 In this era of large machine learning models, distributed training is an essential part of machine learning
 032 pipelines. It can happen in a data center with thousands of connected compute nodes Sergeev & Del Balso
 033 (2018); Huang et al. (2019), or across several data centers and millions of mobile devices in federated learning
 034 Konečný et al. (2016); Kairouz et al. (2019). In such a network, the communication cost is usually the
 035 bottleneck in the whole system. To alleviate the communication burden, and also to preserve privacy to some
 036 extent, one common strategy is to perform multiple local updates before sending the information to other
 037 nodes, which is called Local Gradient Descent (Local-GD) McMahan et al. (2017); Stich (2019); Lin et al.
 038 (2019). In a network with M compute nodes, the goal is to train a global model to fit the distributed datasets:

$$039 \quad \min_{w \in \mathbb{R}^d} f(w) \quad \text{with } f(w) \equiv \frac{1}{M} \sum_{i=1}^M f_i(w), \quad (1)$$

040 where $w \in \mathbb{R}^d$ is the single model to be trained and $f_i(w)$ is the local loss function for i^{th} compute node.
 041 The local loss $f_i(w)$ is the average of the loss function evaluated at model w for the high-dimensional
 042 samples and their corresponding labels, $\{x_s, y_s\}_{s \in S_i}$, where S_i is the local dataset, and $N_i = |S_i|$ is the
 043 number of local samples. The samples of the local dataset are obtained iid from the local distribution D_i .

044 In each round of Local-GD, a central node sends its current model, referred to as the *global model*, to
 045 all compute nodes. Each compute node runs L local gradient descent steps on the global model using
 046 its loss f_i on this model to obtain a local model. Each compute node sends its local model back to the
 047 central node, where these local models are aggregated, by averaging, to obtain the global model for the
 048 next round. The detailed algorithm of Local-GD is described in Algorithms 1.

049 In modern machine learning, most deep neural networks, where Local-GD has impressive performance,
 050 operate in the *overparameterized regime*, where the dimension d of the model is more than the total
 051 number of samples MN . In this case, there are multiple solutions corresponding to zero training loss.
 052 The main question here is:

054 *Q: Which solution would the aggregated model trained by Local-GD converge to?*

055
056 **Contributions.** In this work, we answer this question by analyzing *implicit bias* of Local-GD on classifica-
057 tion tasks for linearly separable data. From the implicit bias of Local-GD, we can characterize the dynamics
058 of the global model across rounds. We compare the global model with the **centralized model** obtained from
059 running gradient descent (GD) on a dataset consisting of all distributed datasets as if all these datasets were
060 located on the central node. The centralized model is obtained from existing results for the implicit bias of
061 linearly separable data Soudry et al. (2018). But these results cannot be directly applied to Local-GD. For
062 globally linearly separable dataset, we show that the global model converges to the centralized model with
063 any arbitrary number of local steps on heterogeneous data. As a consequence of our result on the implicit
064 bias of Local-GD, we can derive the rate of convergence to centralized model as $O(\frac{1}{\log Lk})$, and the training
065 loss converges at the rate of $O(\frac{1}{Lk})$, where k is number of rounds (see Theorems 2) for a constant learning
066 rate $\eta = O(\frac{1}{L})$ (this learning rate is common in existing analysis of distributed learning Karimireddy et al.
067 (2020); Koloskova et al. (2020); Crawshaw et al. (2025)). The meaning of this work lies in: 1). providing
068 a theoretical explanation to the phenomenon that Local-GD can work well with a very large number of
069 local steps in practice; 2). showing the local steps can benefit the convergence rate for smooth, convex
070 functions (such as, logistic loss); this could not be derived from previous analysis in vanilla Local-GD.

071 For a learning rate independent of L , we consider a special case where each local problem with a weakly
072 regularized term is exactly solved, which indicates the behavior of Local-GD with a very large number
073 of local steps. With a Modified Local-GD algorithm (see Section 4.4 we can guarantee that the global
074 model can converge to the centralized model. This result provides the implicit bias of massive local updates
075 without the restrictive learning rate of $O(1/L)$.

076 **Comparisons.** Increasing local steps L does not improve worst-case amount of communication for smooth,
077 convex optimization (Woodworth et al., 2020, Theorem 5), (Koloskova et al., 2020, Theorem 6). For
078 the specific problem of distributed logistic regression, (Crawshaw et al., 2025, Corollary 3) show that a
079 two-stage Local-GD algorithm can improve this worst-case bound. However, their first stage still requires
080 $\eta = O(\frac{1}{L})$, and they can only show that the loss converges, but not the solution the model converges to. In
081 contrast, our Theorem 2 exactly characterizes the global model for Local-GD for any L , and recovers their
082 result as a direct corollary. Another line of work Gu et al. (2023; 2024) approximates Local-Stochastic
083 Gradient Descent (localSGD) by an SDE to obtain an appropriate scaling between L and η . Note that
084 we perform Local-GD with no stochastic noise, and our analysis is exact for finite η . Further, Gu et al.
085 (2023; 2024) do not characterize the exact implicit bias, which we do for linearly separable data. For
086 overparameterized non-linear models, several works Deng et al. (2022b); Song et al. (2023); Maralappanavar
087 et al. (2025) analyze convergence in loss value of Local-GD, but do not provide any guarantees on the global
088 model. Additionally, several works compare the performance of Local-GD and GD on whole dataset Patel
089 et al. (2024); Woodworth et al. (2020) with differences in certain regimes. For overparametrized linear
090 models, we establish that there is no difference between the final model learned by either of these methods.

091 **Practical Implications.** In the existing convergence analysis of Local-GD, the number of local steps L
092 should not be very large for heterogeneous data Stich (2019); Li et al. (2020b). In practical implementation
093 of distributed training on large models, the performance of Local-GD is surprisingly good even with
094 heterogeneous data distribution McMahan et al. (2017); Charles et al. (2021). Also, the number of local
095 steps can be very large in Local-GD type algorithms and real-world systems, for example, up to 500 local
096 steps in distributed training of large language models (LLM) Douillard et al. (2023); Jaghouar et al. (2024).
097 Since our results show the Local-GD can converge to centralized model with *arbitrary* number of local
098 steps, it helps explain why Local-GD can still work well with a large number of local steps in practice.
099 In this work we consider linear models as an appropriate starting point to investigate the implicit bias of
100 Local-GD. A popular example of linear models used in practical machine learning pipelines is fine-tuning
101 last layer on pretrained large models or adding linear layers in transfer learning Donahue et al. (2014);
102 Kornblith et al. (2019) and deployment of LLM Devlin (2018); Jiang et al. (2020). Thus we also add
103 an experiment of fine-tuning last layer of neural network to show broader impact of our analysis.

1.1 RELATED WORK

104 **Convergence of Local-GD.** When data distribution is homogeneous, many works have been done to
105 establish convergence analysis for Local (Stochastic) GD Stich (2019); Yu et al. (2019); Khaled et al. (2020).
106 With a “properly” small number of local steps, the dominating convergence rate is not affected. Further
107 various assumptions have been made to handle data heterogeneity and develop convergence analysis Li et al.

(2020b); Karimireddy et al. (2020); Khaled et al. (2020); Reddi et al. (2021); Wang et al. (2020); Crawshaw et al. (2023). For strongly convex and smooth loss functions, the number of local steps should not be larger than $O(\sqrt{T})$ for i.i.d data Stich (2019) and non-i.i.d. data Li et al. (2020b). However, in practice Local-GD (FedAvg) works well in many applications McMahan et al. (2017); Charles et al. (2021), even in training large language models Douillard et al. (2023); Jaghouar et al. (2024). In Wang et al. (2024), the authors argue that the previous theoretical assumption does not align with practice and proposed a client consensus hypothesis to explain the effectiveness of FedAvg in heterogeneous data. But they do not consider the impact of overparameterization on distributed training. There are some works incorporating the property of zero training loss of overparameterized neural networks into the conventional convergence analysis of FedAvg Huang et al. (2021); Deng et al. (2022a); Song et al. (2023); Qin et al. (2022). However, they do not guarantee which point FedAvg can converge to, which is especially important for overparameterized models since there are multiple solutions with zero training loss. Our work is different from these works as: 1. We analyze which point the Local-GD can converge to, which is a more elementary problem before obtaining the convergence rate; 2. We use implicit bias as a technical tool to analyze the overparameterized FL.

Implicit Bias. Soudry et al. (2018) is the first work to show the gradient descent converges to a max-margin direction on linearly separable data with a linear model and exponentially-tailed loss function. Ji & Telgarsky (2019a) has provided an alternative analysis and extended this to non-separable data. The theory of implicit bias has been further developed, for example, for wide two-layer neural networks Chizat & Bach (2020), deep linear models Ji & Telgarsky (2019b), linear convolutional networks Gunasekar et al. (2018b), two-layer ReLU networks Kou et al. (2024) etc. Beyond gradient descent, more algorithms have been considered, including gradient descent with momentum Gunasekar et al. (2018a), SGD Nacson et al. (2019), Adam Cattaneo et al. (2023), AdamW Xie & Li (2024). Recently, implicit bias has also been used to characterize the dynamics of continual learning, on linear regression Evron et al. (2022); Goldfarb & Hand (2023); Lin et al. (2023), and linear classification Evron et al. (2023); Jung et al. (2025). In Evron et al. (2023), gradient descent on continually learned tasks is related to Projections onto Convex Sets (POCS) and shown to converge to a *sequential* max-margin scheme. In our work we consider the implicit bias of gradient descent in distributed setting, which is related to a different parallel projection scheme by projecting onto constraint sets *simultaneously*.

Parallel Projection. Parallel projection methods are a family of algorithms to find a common point across multiple constraint sets by projecting onto these sets in parallel. These methods are widely used in feasibility problems in signal processing and image reconstruction Bauschke & Combettes (2011). The straightforward average of multiple projections is known as the simultaneous iterative reconstruction technique (SIRT) in Gilbert (1972). Then de Pierro & Iusem (1984) studied the convergence of PPM for a relaxed version, and Combettes (1994) further generalized the result to inconsistent feasibility problems. In Combettes (1997), an extrapolated parallel projection method was proposed to accelerate the convergence. We note that Jhunjhunwala et al. (2023) used this extrapolation to accelerate FedAvg. However, it was just inspired by the similarity between parallel projection method and FedAvg, while in this work we rigorously prove the relation between PPM and FedAvg using implicit bias of gradient descent.

Algorithm 1 LOCAL-GD.

```

1: Input: learning rate  $\eta$ .
2: Initialize  $w_0^0$ 
3: for  $k=0$  to  $K-1$  do
4:   The aggregator sends global model  $w_0^k$  to all compute nodes.
5:   for  $i=1$  to  $i=M$  do
6:     compute node  $i$  updates local model starting from  $w_0^k$ :  $w_i^{k,0} = w_0^k$ .
7:     for  $l=0$  to  $L-1$  do
8:        $w_i^{k,l+1} = w_i^{k,l} - \eta \nabla f_i(w_i^{k,l})$ .
9:     end for
10:    compute node  $i$  sends back the updated local model  $w_i^{k+1} = w_i^{k,L}$ .
11:  end for
12:  The aggregator aggregates all the local models:  $w_0^{k+1} = \frac{1}{M} \sum_{i=1}^M w_i^{k+1}$ .
13: end for
14: Output:  $w_0^K$ .

```

162 **2 MOTIVATING OBSERVATION IN LINEAR REGRESSION**
163

164 In this section we first give some observations in linear regression as a motivating example. The behavior
165 of linear regression is very well-understood in high-dimensional statistics.

166 **Setting:** At each compute node i , the dataset S_i consists of N tuples of samples and their corresponding la-
167 bels, $(x, y) \in \mathbb{R}^d \times \mathbb{R}$. Denote $X_i = [x_{i1}, x_{i2}, \dots, x_{iN}]^T \in \mathbb{R}^{N \times d}$ as the data matrix at i -th compute node, and
168 $y_i = [y_{i1}, y_{i2}, \dots, y_{iN}]^T \in \mathbb{R}^N$ as the label vector. Let $X_c = [X_1^T, \dots, X_M^T]^T \in \mathbb{R}^{MN \times d}$ be the data matrix con-
169 sisting of all the local data, and $y_c = [y_1^T, \dots, y_M^T]^T \in \mathbb{R}^{MN \times 1}$ be the label vector consisting of the local labels.
170

171 We consider a special case of Local-GD in Algorithm 1 where the number of local steps is very large.
172 At each round, the aggregator sends the global model w_0 to all the compute nodes. Each compute node
173 minimizes the squared loss $f_i(w_i) = \frac{1}{2N} \|y_i - X_i w_i\|^2$ by a large number of gradient descent steps until
174 convergence. Then each compute node sends back the local model and the aggregator aggregates all the
175 local models to get the updated global model.

176 **Underparameterized Regime:** When the number of local samples is larger than the dimension d , it is
177 known that local model would converge to the ordinary least square solution $w_i^{k+1} = (X_i^T X_i)^{-1} X_i^T y_i$
178 regardless of initial point w_i^k . In the meanwhile, the centralized model with all the training samples
179 is $w_c = (X_c^T X_c)^{-1} X_c^T y_c$. However, the average of local models $w_0 = \sum_{i=1}^M (X_i^T X_i)^{-1} X_i^T y_i$ is not
180 identical to the centralized model unless the data is homogeneously distributed and all $X_i^T X_i$ are
181 proportional. So a large number of local steps can hurt the convergence to centralized model with
182 heterogeneous data distribution.

183 **Overparameterized Regime:** When the dimension is larger than the number of samples at each compute
184 node ($d > N$), there are multiple solutions corresponding to zero squared loss. However, it is known that
185 gradient descent would converge to the minimum norm solution in the feasible set, which corresponds
186 to a minimum Euclidean distance to the initial point Gunasekar et al. (2018a); Evron et al. (2022), i.e.,
187 the solution of the optimization problem

188
$$\min_{w_i} \|w_i - w_0^k\|^2 \quad \text{s.t.} \quad X_i w_i = y_i. \quad (2)$$
189

190 We can obtain the closed form solution as $w_i^{k+1} = (I - P_i)w_0^k + X_i^\dagger y_i$, where $P_i \triangleq X_i^T (X_i X_i^T)^{-1} X_i$ and
191 $X_i^\dagger \triangleq X_i^T (X_i X_i^T)^{-1}$. We observe that P_i is the projection operator to the row space of X_i , and X_i^\dagger is
192 the pseudo inverse of X_i . Meanwhile the centralized model converges to the minimum norm solution
193 $w_c = X_c^T (X_c X_c^T)^{-1} y_c$. Denote $\bar{P} = \frac{1}{M} \sum_{i=1}^M P_i$. In the training process the difference between global
194 model and centralized model is iteratively projected onto the null space of span of row spaces of X_i s. It
195 implies that the difference on the span of data matrix gradually decreases until zero. Based on the evolution
196 of the difference, we can prove the following theorem:

197 **Theorem 1.** For the linear regression problem, suppose the initial point w_0^0 is 0 and $d > MN$ and the min-
198 imum eigenvalue θ_{\min} of \bar{P} is larger than 0, then the output of Local-GD, w_0^K , converges to the centralized
199 solution w_c as the number of communication rounds $K \rightarrow \infty$ as $\|w_0^K - w_c\| \leq (1 - \theta_{\min})^K \|w_c\|$.

200 The proof is deferred in Appendix B. The key step is to show the initial difference is already in the data
201 space, and no residual in the null space of row spaces of X_i s. The convergence to the centralized model is at
202 exponential rate. Due to the linearity of the regression problem, we can theoretically show the global model
203 can exactly converge to the centralized model with implicit bias on overparameterized regime. It implies
204 that, even if we use a large number of local steps to exactly solve the local problems on very heterogeneous
205 data, the performance of Local-GD is equivalent to train a model with all the data in one place.

207 **3 IMPLICIT BIAS OF LOCAL-GD FOR CLASSIFICATION**
208

209 For classification task, we also would like to know whether the global model can converge to the centralized
210 model with any number of local steps. Now we investigate a binary classification task with linear models.
211

212 **3.1 SETTING**
213

214 Suppose, for each compute node i , the dataset S_i consists of N_i tuples of samples and their corresponding
215 labels, $(x, y) \in \mathbb{R}^d \times \{+1, -1\}$. We denote $X_i \in \mathbb{R}^{N_i \times d}$ as the data matrix at i -th compute node, and
 $y_i \in \{+1, -1\}^{N_i}$ as the label vector. The global dataset is the set of M local datasets $S = \bigcup_{i=1}^M S_i$.

216 We consider a linear model $w \in \mathbb{R}^d$ for the binary classification task. The local loss at i -th compute node is
 217

$$218 \quad 219 \quad f_i(w) = \sum_{s \in S_i} g(y_s x_s^T w), \quad (3)$$

220 where $g(u)$ is a loss function decreasing to zero when $u \rightarrow \infty$, such as logistic loss $g(u) = \ln(1 + e^{-u})$.
 221

222 We study LocalGD with an *arbitrary number* of gradient descent steps. To describe our main results, we
 223 have the following notations and assumptions. We denote the whole data matrix as $X \in \mathbb{R}^{N \times d}$, where
 224 $N = \sum_{i=1}^M N_i$. We write $\sigma_{\max} = \sqrt{\theta_{\max}(X^T X)}$ as the maximum singular value of data matrix X , where
 225 θ represents eigenvalues of a square matrix. We need an assumption of global separability on whole dataset.

226 **Assumption 1.** For all the data samples $(x_s, y_s) \in S$, there exists $w \in \mathbb{R}^d$ such that $y_s x_s^T w > 0$.
 227

228 Note that linear separability is a common assumption in the analysis of learning in overparameterized
 229 regime Nacson et al. (2019); Soudry et al. (2018); Evron et al. (2023). For our distributed case, this
 230 implies that all clients share at least 1 minimizer, which imposes an extremely mild condition on the data
 231 heterogeneity among clients. In the overparametrized setting, $d \geq mn$, hence, there are likely several such
 232 solutions separating the whole dataset. Since there are multiple solutions separating the whole dataset,
 233 we define a particular max-margin solution on global dataset:

$$234 \quad 235 \quad \hat{w} = \arg \min_{w \in \mathbb{R}^d} \|w\| \quad \text{s.t.} \quad y_s x_s^T w \geq 1, \quad \forall s \in S. \quad (4)$$

236 It has been proven that gradient descent would implicitly lead the linear model to this max-margin solution
 237 in direction, i.e., convergence of model direction to $\hat{w}/\|\hat{w}\|$ Soudry et al. (2018). We define the maximum
 238 margin as

$$239 \quad 240 \quad \gamma = \max_{w \in \mathbb{R}^d, \|w\|=1} \min_s y_s x_s^T w \quad (5)$$

241 which is strictly positive since the global dataset is linearly separable. The data points reaching this margin
 242 are support vectors of the global dataset.
 243

244 To establish convergence, we require additional regularity assumptions on the loss function.

245 **Assumption 2.** The loss function $g(u)$ is a positive, differentiable, β -smooth function, monotonically
 246 decreasing to zero, and $\limsup_{u \rightarrow -\infty} g' < 0$.

247 **Assumption 3.** The negative loss derivative $-g'(u)$ has a tight exponential tail. That is, there exists
 248 positive constants μ_+, μ_- and \bar{u} such that $\forall u > \bar{u}$:

$$249 \quad 250 \quad (1 - \exp(-\mu_- u)) e^{-u} \leq -g'(u) \leq (1 + \exp(-\mu_+ u)) e^{-u}. \quad (6)$$

251 Note that these assumptions are also used in centralized learning of overparameterized models Soudry
 252 et al. (2018); Nacson et al. (2019); Evron et al. (2023), and the logistic loss satisfies all the assumptions.
 253 With our setting completely defined, we state our main results.
 254

255 3.2 LOSS CONVERGENCE AND IMPLICIT BIAS OF LOCAL-GD 256

257 Our main result is on the asymptotic convergence of the model parameter w_0 and loss $f(w)$ for Local-GD.

258 **Theorem 2.** Under assumptions 1, 2, 3, if the learning rate satisfies $\eta < \min\left(\frac{1}{2L\sigma_{\max}^2\beta}, \frac{\gamma^2}{4L\sigma_{\max}^3\beta(\gamma+\sigma_{\max})}\right)$,
 259 then for the process of Local-GD, we have,

- 260 • Every data point is classified correctly finally: $\lim_{k \rightarrow \infty} x_s^T w_0^k = \infty, \forall s \in S$.
- 261 • The global model obtained from Local-GD will behave as

$$262 \quad 263 \quad w_0^k = \log(Lk) \hat{w} + \rho^k, \quad \text{and,} \quad \left\| \frac{w_0^k}{\|w_0^k\|} - \frac{\hat{w}}{\|\hat{w}\|} \right\| = O\left(\frac{1}{\log Lk}\right) \quad (7)$$

264 and $\|\rho^k\| < \infty$ for all k . This implies, the normalized global model converges to the global
 265 max-margin solution.

- 266 • The loss function $f(w_0^k)$ decreases to zero as $f(w_0^k) = O\left(\frac{1}{Lk}\right)$.

270 The proof is deferred to Appendix C. The technical challenges lie in that we need to control the residual term
 271 ρ^k with the *local steps* and *aggregations*, which are handled by a refined analysis in distributed context. This
 272 theorem implies the global model can eventually correctly classify all the training samples after many rounds
 273 of communication. Given that centralized model also converges to the global max-margin solution from
 274 prior results, the global model from Local-GD actually converges to the exact centralized model in direction.
 275 Further, this holds for a step size $\eta \propto \frac{1}{L}$, and does not require any additional modifications to the objective,
 276 for instance, any regularization on the difference between local and global models during local steps.

277 **Impact of local steps.** In this analysis, the number of local steps can be arbitrary. Although the magnitude
 278 of model vector would diverge to infinity, the direction of aggregated model still converges to the direction
 279 of global max-margin solution. Thus, the number of local steps does not influence the asymptotic
 280 convergence to the centralized model, which is very different from underparameterized regime. This result
 281 also shows the local steps can be beneficial for convergence to the global max-margin solution as both
 282 the loss and the directional error decrease with total number of gradient descent steps (Lk) at rates $\frac{1}{Lk}$ and
 283 $\frac{1}{\log(Lk)}$ respectively. Additionally, our convergence rates also match those obtained for GD in centralized
 284 learning Soudry et al. (2018) with total number of steps Lk . This demonstrates that our analysis is tight.
 285 Further, for constant γ , if we use the same number of local steps, $L = \Theta(\sqrt{\frac{M}{\epsilon}})$ as two-stage Local-GD in
 286 (Crawshaw et al., 2025, Corollary 3), then we require the same number of rounds $\mathcal{O}(\sqrt{\frac{M}{\epsilon}})$ of Local-GD
 287 to achieve $f(w_0^k) \leq \epsilon$. Note that both Crawshaw et al. (2025) as well as our Theorem 2 require the number
 288 of rounds to be larger than some \bar{k} after which asymptotics kick in. Therefore, we assume that ϵ is small
 289 enough that the number of rounds to be $\mathcal{O}(\sqrt{\frac{M}{\epsilon}})$ is much larger than this \bar{k} .
 290

291 **Learning Rate.** Theorems 2 needs the learning rate to be small as $O(1/L)$, which has also been used by
 292 existing works Karimireddy et al. (2020); Koloskova et al. (2020); Crawshaw et al. (2025) on Local-GD and
 293 Local-SGD. This means the model does not move so far after one round of local iterations. Next, we would
 294 see whether the global model still converges to max-margin solution with a learning rate independent of L .
 295

297 3.3 DISCUSSIONS

298 **Extension to Local SGD.** It is straightforward to extend our analysis of Local-GD to Local SGD
 299 that chooses samples without replacement. At each local step of i -th compute node, the update is
 300 $w_i^{k,l+1} = w_i^{k,l} - \eta \frac{1}{B} \sum_{s \in S_{i,l}} \nabla g(y_s x_s^T w_i^{k,l})$, where $S_{i,l}$ is the mini-batch of samples at l -th local step and
 301 $B = |S_{i,l}|$ is the batch size. We consider the following setting of sampling:
 302

303 **Assumption 4** (Sampling without replacement.). At every communication round, each compute node
 304 run stochastic gradient descent with E epochs, where E is an positive integer. Within each epoch, the
 305 mini-batches $\{S_{i,0}, S_{i,1}, \dots, S_{i,l'}\}$ partition the local dataset S_i , where $l' = N/B$ is the number of local steps
 306 for one epoch.
 307

308 Under this setting, each sample is exactly chosen once inside one epoch of local updates. At each round,
 309 the local datasets are passed E times, which is a practically common way. To extend our analysis to
 310 Local SGD, we can regard one local dataset as a “batch” in SGD for sampling without replacement. And
 311 then we perform multiple gradient steps in the same “batch”, not only one step of gradient descent in
 312 SGD. In Local SGD, each step is a gradient descent step on a mini batch of local datasets, but we still
 313 run the gradient descent steps for E “local steps”. Therefore, we can obtain the same asymptotic results
 314 as Theorem 2 for Local SGD without any change of the proof framework.
 315

316 **Separability Assumption.** In this paper we mainly focus on the linearly separable data, which is a
 317 standard assumption in implicit bias analysis and also widely used in recent works Zhang et al. (2024);
 318 Crawshaw et al. (2025); Jung et al. (2025). For non-separable case, Ji & Telgarsky (2019a) has shown
 319 gradient descent converges to a ray along the direction of max-margin solution of largest linearly separable
 320 subset. However, there is still an assumption on the data: in fact, one needs a positive margin on the
 321 separable part of data to show both convergence in risk or parameters. Nevertheless, Ji & Telgarsky (2019a)
 322 clearly shows strict linear separability is not the main reason for the convergence of gradient descent
 323 to a max-margin solution. Since even without this assumption, GD still converges to a variant form of
 324 max-margin solution. It is possible to use the same idea in Local-GD. Intuitively, in the case where local
 325 datasets are linearly separable but global dataset is non-separable, although local training would guide local

324 models to local max-margin solutions, the aggregations would force the global model to converge to the
 325 max-margin solution of largest linearly separable subset of global dataset, which is the centralized solution.
 326

327 4 IMPLICIT BIAS OF LOCAL-GD WITH LEARNING RATE INDEPENDENT OF L

328 4.1 SETTING

331 In this section, we consider Local-GD in a slightly different setting. We aim to solve a local optimization
 332 problem with exponential loss and a weakly regularized term for each compute node. The local problem
 333 is solved exactly (to reach the local optima) with a large number of local steps.

334 **Algorithm.** At each round, the aggregator sends the global model w_0 to all the compute nodes. Each
 335 compute node minimizes an *exponential loss* with a *weakly regularized term* by many gradient descent
 336 steps *until convergence*. That is, each compute node solves the following problem:
 337

$$338 \min_{w \in \mathbb{R}^d} f_i(w) \quad \text{where } f_i(w) \equiv \sum_{s \in S_i} \exp(-y_s x_s^T w) + \frac{\lambda}{2} \|w - w_0^k\|^2 \quad (8)$$

340 where λ is a regularization parameter close to 0.

342 Then each compute node sends back the local model and the aggregator aggregates all the local models
 343 to get the updated global model (i.e., they follow Algorithm 1 with $f_i(w_i)$ as specified here).

344 Regularization methods are very common in distributed learning to force the local models move not too far
 345 from global model Li et al. (2020a; 2021); T Dinh et al. (2020). Here we consider the weakly regularized
 346 term, $\lambda \rightarrow 0$, to give theoretical insights of Local-GD on classification tasks. Experimentally the λ is set
 347 to be extremely small that does not affect the minimization of exponential loss. For the local loss functions,
 348 we have one assumption on smoothness:

349 **Assumption 5.** For each compute node, the local loss function $f_i(w)$ is B -smooth for any round of local
 350 steps k .
 351

352 **Learning Rate.** In the following analysis of implicit bias, we actually exploit the property of local
 353 minimizers. Since local problem (8) is a strongly convex problem for $\lambda > 0$, we can run local gradient
 354 descent to find the unique minimizer with a learning rate $\eta \leq \frac{2}{B}$ for a large number of local steps L . That's
 355 the only requirement of learning rate, which is not dependent of number of local steps L . In other words, the
 356 learning rate is only needed to be sufficiently small to ensure local convergence at each round of Local-GD.

357 4.2 IMPLICIT BIAS OF LOCAL-GD AND RELATION TO PPM

360 We consider the whole algorithmic process of Local-GD on classification and use another auxiliary
 361 sequence of global models, denoted as $\bar{w}_0^k, k=0,1,2,\dots$. Starting from an initial point \bar{w}_0^0 , the central node
 362 sends global model \bar{w}_0^k to all the compute nodes at k -th iteration round. Each compute node solves the
 363 following *Local Max-Margin* problem to obtain \bar{w}_i^{k+1} :

$$364 \bar{w}_i^{k+1} = \arg \min_{w \in \mathbb{R}^d} \|w - \bar{w}_0^k\| \quad \text{s.t.} \quad y_s x_s^T w \geq 1, \quad \forall s \in S_i. \quad (9)$$

366 Then the compute node sends the local model back. The central node averages the local models to get
 367 $\bar{w}_0^{k+1} = \frac{1}{M} \sum_{i=1}^M \bar{w}_i^{k+1}$. We can show the solution w_0^K obtained in Local-GD converges in direction to
 368 the global model from Local Max-Margin problems \bar{w}_0^K .

369 **Lemma 1.** For almost all datasets sampled from a continuous distribution satisfying Assumption 1, with
 370 initialization $w_0^0 = \bar{w}_0^0 = 0$, we have $w_0^k \rightarrow \ln\left(\frac{1}{\lambda}\right) \bar{w}_0^k$, and the residual $\|w_0^k - \ln\left(\frac{1}{\lambda}\right) \bar{w}_0^k\| = O(k \ln \ln \frac{1}{\lambda})$,
 371 as $\lambda \rightarrow 0$. It implies that at any round $k = o\left(\frac{\ln(1/\lambda)}{\ln \ln(1/\lambda)}\right)$, w_0^k converges in direction to \bar{w}_0^k :

$$374 \lim_{\lambda \rightarrow 0} \frac{w_0^k}{\|w_0^k\|} = \frac{\bar{w}_0^k}{\|\bar{w}_0^k\|}. \quad (10)$$

376 The proof is deferred in Appendix D. The proof sketch is similar to the continual learning work Evron
 377 et al. (2023), but we have to handle the parallel local updates for each dataset from the same initial model

378 and the aggregation, which is different from the sequential updates where for each dataset the model is
 379 trained from the previous model and there is no need to do aggregation.
 380

381 Based on this equivalence between Local-GD for linear classification and Local Max-Margin scheme,
 382 we can further analyze the performance of Local-GD with a large number of local steps. Instead of a
 383 closed-form solution for the Local Max-Margin problem (9), we treat it as a projection of the aggregated
 384 global model onto a convex set C_i : $\bar{w}_i^{k+1} = P_i(\bar{w}_0^k)$, which is formed by the constraints in (9) and exactly
 385 the local feasible set defined in Assumption 1. Here we slightly overload the notation P_i , which was used
 386 as the projection matrix in linear regression since the readers can get a sense of the same effect of them
 387 in Local-GD. The aggregation is actually to average the local projected points: $\bar{w}_0^{k+1} = \frac{1}{M} \sum_{i=1}^M P_i(\bar{w}_0^k)$.
 388

389 The sequence of Local Max-Margin schemes is therefore projections to local (convex) feasible sets
 390 followed by aggregation, which is the Parallel Projection Method (PPM) in literature Gilbert (1972);
 391 Combettes (1994). Using Lemma 1, we establish the relation between Local-GD and PPM: the model
 392 from Local-GD converges to the model from PPM in direction.

393 4.3 CONVERGENCE TO GLOBAL FEASIBLE SET

394 Now we use the properties of PPM to characterize the performance of Local-GD in classification. In
 395 Combettes (1994), the convergence of PPM has been provided for a relaxed version. The direct average
 396 considered in this work can be seen as a special case of the relaxed version, and the following lemma holds.
 397

398 **Lemma 2** (Theorem 1 and Proposition 8, Combettes (1994)). *Suppose all the local feasible sets
 399 $C_i, i=1, 2, \dots$ are closed and convex, and the intersection \bar{C} is not empty. Then for any initial point \bar{w}_0^0 ,
 400 the global model \bar{w}_0 generated by PPM converges to a point in the global feasible set \bar{C} .*

401 This lemma guarantees that \bar{w}_0^K will converge to the intersection of the convex sets after many rounds
 402 of iteration, however we are not sure which exact point it would converge to.

403 Combining Lemma 1, Lemma 2 and the fact that centralized model would converge to the minimum norm
 404 solution in global feasible set, we immediately have:

405 **Theorem 3.** *For linear classification problem with exponential loss, suppose initial point is $w_0^0 = 0$. The
 406 aggregated global model w_0^K obtained by Local-GD with a large number of local steps converges in
 407 direction to one point in the global feasible set \bar{C} , while the centralized model converges in direction to
 408 the minimum norm point in the same set.*

409 Here we cannot guarantee the global model obtained by Local-GD with a learning rate independent of L
 410 to converge exactly to the centralized model in classification, but show that it converges to the same global
 411 feasible set as the centralized solution. To theoretically support that the Local-GD model converges to
 412 the centralized model, we propose a slightly Modified Local-GD by just changing the aggregation method,
 413 and showing that it converges to the centralized model exactly.

415 4.4 MODIFIED LOCAL-GD: CONVERGENCE TO CENTRALIZED MODEL

417 In Combettes (1996) it was shown that if the aggregation method is modified to incorporate the influence
 418 of the initial point \bar{w}_0^0 in PPM, then the sequence generated by PPM will converge to a specific point in
 419 global feasible set \bar{C} with minimum distance to this initial point. Denote $P_c(\cdot)$ as the projection operator
 420 onto the global feasible set \bar{C} . Formally we have the following lemma.

421 **Lemma 3** (Theorem 5.3, Combettes (1996)). *Suppose \bar{C} is not empty. For any initial point \bar{w}_0^0 , when
 422 the local models are aggregated as*

$$424 \quad \bar{w}_0^{k+1} = (1 - \alpha^{k+1}) \bar{w}_0^0 + \alpha^{k+1} \left(\frac{1}{M} \sum_{i=1}^M P_i(\bar{w}_0^k) \right), \quad (11)$$

427 where $\{\alpha^k\}$ satisfy (i) $\lim_{k \rightarrow \infty} \alpha^k = 1$, (ii) $\sum_{k \geq 0} (1 - \alpha^k) = \infty$, (iii) $\sum_{k \geq 0} |\alpha^{k+1} - \alpha^k| < \infty$, then the
 428 global model generated by PPM will converge to the point $P_c(\bar{w}_0^0)$.
 429

430 The sequence generated by PPM would converge to the point in global feasible set, \bar{C} , with minimum
 431 distance to \bar{w}_0^0 . The modified aggregation method is a linear combination of initial point and current average
 432 of local projected points. One example of the sequence $\{\alpha^k\}$ satisfying the conditions is $\alpha^k = 1 - \frac{1}{k+1}$.

If we start from $\bar{w}_0^0 = 0$, then the point $P_c(\bar{w}_0^0)$ is exactly the minimum norm point in the global feasible set. It shows the PPM can exactly converge to the minimum norm point as the centralized model. Based on this result, we propose a Modified Local-GD algorithm, with the replacement of Line 9 in Algorithm 1 with

$$w_0^{k+1} = (1 - \alpha^k)w_0^k + \alpha^k \left(\frac{1}{M} \sum_{i=1}^M w_i^k \right). \quad (12)$$

We still need to prove a lemma analogous to Lemma 1 to establish the equivalence between Modified Local-GD and Modified PPM, which is omitted here due to space limit (Please refer to Appendix D and the proof is very similar to proof in Lemma 1). From the equivalence, Lemma 3, and implicit bias of the centralized model, we can have the following theorem:

Theorem 4. *For linear classification problem with local loss (8), suppose the initial point is $w_0^0 = 0$. Then the global model w_0^K obtained by Modified Local-GD converges in direction to the centralized model obtained from (4).*

Unlike the vanilla Local-GD, which is only guaranteed to converge to the global feasible set, the Modified Local-GD is guaranteed to converge to the centralized model in direction. Note that if we start from $\bar{w}_0^0 = 0$, the aggregation in Modified Local-GD becomes $w_0^{k+1} = \frac{k}{k+1} \left(\frac{1}{M} \sum_{i=1}^M w_i^k \right)$, which is just a scaling of vanilla aggregation with a parameter less than 1. Thus we can see experimentally they usually converge to the same point and Modified Local-GD converges slightly slower. With Modified Local-GD, we can theoretically show the global model still converges to centralized model in direction with a learning rate independent of L .

5 EXPERIMENTS

We conducted various experiments on linear classification and neural network fine-tuning. We compared the **global model**, i.e., the output of Local-GD (Algorithm 1), with the **centralized model**, i.e., the model obtained from running GD on a dataset consisting of all distributed datasets at one place, in different scenarios.

5.1 LINEAR CLASSIFICATION

For linear classification, we have 10 compute nodes with 50 training samples at each. The dataset is generated as $y_{ij} = \text{sign}(x_{ij}^T w_i^*)$, where ground truth model is $w_i^* = w^* + z_i$, and w^* is a Gaussian vector randomly chosen, z_i is a Gaussian noise. The data matrix X_i is a Gaussian matrix. This setting makes sure the datasets across compute nodes are different from each other, meanwhile they are not totally different such that there may be a non-empty global feasible set.

We tested four models for linear classification. The global model (G) is trained exactly with Local-GD and logistic loss. The centralized model (C) is trained with gradient descent on the global dataset. The global model from Modified Local-GD (G-Mod) is trained with exponential loss and regularization term as $\lambda = 0.0001$. The centralized SVM model (S) (max-margin solution) is obtained by solving problem (4) via standard scikit-learn package. Note that centralized model and SVM model are the final trained model in the plots. The learning rate of (local) gradient descent is $\eta = 0.01$. Since our theory claimed the convergence is established in direction, the difference here for two models w_1, w_2 is defined after normalization $\|w_1/\|w_1\| - w_2/\|w_2\|\|$.

In Fig. 1(a), we show the difference between global model from Local-GD and centralized model with different number of local steps. The model dimension is chosen as $d = 1500$, ensuring it is globally over-parameterized. The centralized model is trained with 20000 gradient descent steps. It is seen the difference can approach zero for all the L , and larger L can result in faster convergence to the centralized model.

In Figs. 1(b), 1(c), 1(d), the number of local steps is fixed as $L = 150$ for Local-GD and Modified Local-GD, and the number of communication rounds is fixed as $R = 120$ for all the dimensions. Fig. 1(b) shows the difference between these models with respect to the number of rounds R when dimension is $d = 1500$. We can see both global model and modified global model converges to the centralized model in direction, and the centralized model is close to the SVM model but there is small gap. Fig. 1(c) displays the difference with respect to dimension d . It is seen the difference between global model and centralized model gradually decreases with larger dimensions. The modified global model is almost the same as

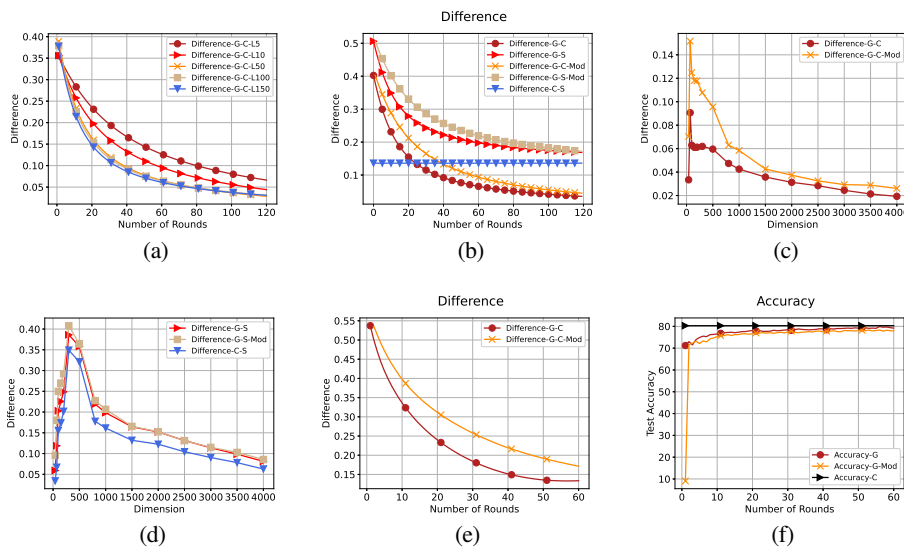


Figure 1: (a) Difference between global model and centralized model with L . (b) Difference between global model and centralized model with R . (c) Difference between global model and centralized model with d . (d) Difference from SVM model with d . (e) Difference between global linear layer and centralized linear layer with R . (f) Test accuracy of neural network fine-tuning.

the centralized model but the gap is slightly larger since it converges slower than vanilla global model with same number of rounds. Fig. 1(d) shows the difference from SVM model with dimension. The gap between the models to SVM model also decreases with larger d .

5.2 FINE-TUNING OF PRETRAINED NEURAL NETWORK

We further fine-tuned the ResNet50 model pretrained with ImageNet dataset on CIFAR10 dataset. Only the final linear layer is trained during the process, while the rest of model is fixed. The 50000 samples are distributed on 10 compute nodes. For i -th compute node, the half of local dataset belongs to the same class, and the other half consists of rest of 9 classes evenly, which forms a heterogeneous data distribution. The centralized model is trained with the whole CIFAR10 dataset. The models are trained with cross entropy loss and Local SGD. The learning rate is 0.01 and the batch size is 128. The number of local steps is $L=60$ and number of communication rounds is $R=60$. The centralized model is trained with the same learning rate for 3600 steps. We plot the difference between the linear layer and test accuracy with number of rounds in Fig. 1(e) and 1(f). Again the difference is defined in direction. We can see the difference gradually decreases to a small error floor and the accuracy of global models and centralized model is very similar at last.

Due to page limit, we put more experimental results on linear regression, linear classification with Dirichlet distribution in Appendix A.

6 CONCLUSIONS

In this work we analyzed the implicit bias of GD in distributed setting, and characterized the dynamics of the global model trained from Local-GD. We showed that Local-GD can converge to a centrally trained model for linearly separable data with a constant learning rate $O(1/L)$, and a Modified Local-GD can have the same convergence for a learning rate independent of L . Our analysis provided a new perspective why Local-GD works well in practice even with a large number of local steps on heterogeneous data.

540 REPRODUCIBILITY STATEMENT
541542 This paper is mainly a theoretical work. The assumptions 1-5 are clearly explained in the main text. The
543 proofs of Section 2 are included in Appendix B. The proof of Theorem 2 is included in Appendix C. The
544 proofs of lemmas and theorems in Section 4 are included in Appendix D.
545546 REFERENCES
547548 Heinz H Bauschke and Patrick L Combettes. *Convex Analysis and Monotone Operator Theory in Hilbert*
549 *Spaces*. Springer, 2011.551 Matias D Cattaneo, Jason M Klusowski, and Boris Shigida. On the implicit bias of adam. *arXiv preprint*
552 *arXiv:2309.00079*, 2023.553 Zachary Charles, Zachary Garrett, Zhouyuan Huo, Sergei Shmulyan, and Virginia Smith. On large-cohort
554 training for federated learning. *Advances in neural information processing systems*, 34:20461–20475,
555 2021.557 Hong-You Chen and Wei-Lun Chao. Fedbe: Making bayesian model ensemble applicable to federated
558 learning. In *International Conference on Learning Representations*, 2021.559 Lenaic Chizat and Francis Bach. Implicit bias of gradient descent for wide two-layer neural networks
560 trained with the logistic loss. In *Conference on learning theory*, pp. 1305–1338. PMLR, 2020.562 Patrick L Combettes. Inconsistent signal feasibility problems: Least-squares solutions in a product space.
563 *IEEE Transactions on Signal Processing*, 42(11):2955–2966, 1994.564 Patrick L Combettes. The convex feasibility problem in image recovery. In *Advances in imaging and*
565 *electron physics*, volume 95, pp. 155–270. Elsevier, 1996.567 Patrick L Combettes. Convex set theoretic image recovery by extrapolated iterations of parallel subgradient
568 projections. *IEEE Transactions on Image Processing*, 6(4):493–506, 1997.570 Michael Crawshaw, Yajie Bao, and Mingrui Liu. Federated learning with client subsampling, data
571 heterogeneity, and unbounded smoothness: A new algorithm and lower bounds. *Advances in Neural*
572 *Information Processing Systems*, 36, 2023.573 Michael Crawshaw, Blake Woodworth, and Mingrui Liu. Local steps speed up local GD for heterogeneous
574 distributed logistic regression. In *The Thirteenth International Conference on Learning Representations*,
575 2025. URL <https://openreview.net/forum?id=lydPkW4lfz>.577 Alvaro Rodolfo de Pierro and Alfredo Noel Iusem. *A parallel projection method of finding a common point*
578 *of a family of convex sets*. Inst. de matemática pura e aplicada, Conselho nacional de desenvolvimento . . .,
579 1984.580 Yuyang Deng, Mohammad Mahdi Kamani, and Mehrdad Mahdavi. Local sgd optimizes overparameterized
581 neural networks in polynomial time. In *International Conference on Artificial Intelligence and Statistics*,
582 pp. 6840–6861. PMLR, 2022a.584 Yuyang Deng, Mohammad Mahdi Kamani, and Mehrdad Mahdavi. Local sgd optimizes overparameterized
585 neural networks in polynomial time. In Gustau Camps-Valls, Francisco J. R. Ruiz, and Isabel Valera
586 (eds.), *Proceedings of The 25th International Conference on Artificial Intelligence and Statistics*, volume
587 151 of *Proceedings of Machine Learning Research*, pp. 6840–6861. PMLR, 28–30 Mar 2022b. URL
588 <https://proceedings.mlr.press/v151/deng22a.html>.589 Jacob Devlin. Bert: Pre-training of deep bidirectional transformers for language understanding. *arXiv*
590 *preprint arXiv:1810.04805*, 2018.592 Jeff Donahue, Yangqing Jia, Oriol Vinyals, Judy Hoffman, Ning Zhang, Eric Tzeng, and Trevor Darrell.
593 Decaf: A deep convolutional activation feature for generic visual recognition. In *International*
594 *conference on machine learning*, pp. 647–655. PMLR, 2014.

594 Arthur Douillard, Qixuan Feng, Andrei A Rusu, Rachita Chhaparia, Yani Donchev, Adhiguna Kuncoro,
 595 Marc'Aurelio Ranzato, Arthur Szlam, and Jiajun Shen. Diloco: Distributed low-communication training
 596 of language models. *arXiv preprint arXiv:2311.08105*, 2023.

597 Itay Evron, Edward Moroshko, Rachel Ward, Nathan Srebro, and Daniel Soudry. How catastrophic can
 598 catastrophic forgetting be in linear regression? In *Conference on Learning Theory*, pp. 4028–4079.
 599 PMLR, 2022.

600 Itay Evron, Edward Moroshko, Gon Buzaglo, Maroun Khriesh, Badea Marjeh, Nathan Srebro, and Daniel
 601 Soudry. Continual learning in linear classification on separable data. *arXiv preprint arXiv:2306.03534*,
 602 2023.

603 Peter Gilbert. Iterative methods for the three-dimensional reconstruction of an object from projections.
 604 *Journal of theoretical biology*, 36(1):105–117, 1972.

605 Daniel Goldfarb and Paul Hand. Analysis of catastrophic forgetting for random orthogonal transformation
 606 tasks in the overparameterized regime. In *International Conference on Artificial Intelligence and
 607 Statistics*, pp. 2975–2993. PMLR, 2023.

608 Xinran Gu, Kaifeng Lyu, Longbo Huang, and Sanjeev Arora. Why (and when) does local SGD generalize
 609 better than SGD? In *The Eleventh International Conference on Learning Representations*, 2023. URL
 610 <https://openreview.net/forum?id=svCcui6Drl>.

611 Xinran Gu, Kaifeng Lyu, Sanjeev Arora, Jingzhao Zhang, and Longbo Huang. A quadratic synchronization
 612 rule for distributed deep learning. In *The Twelfth International Conference on Learning Representations*,
 613 2024. URL <https://openreview.net/forum?id=yroyhkhWS6>.

614 Suriya Gunasekar, Jason Lee, Daniel Soudry, and Nathan Srebro. Characterizing implicit bias in terms of op-
 615 timization geometry. In *International Conference on Machine Learning*, pp. 1832–1841. PMLR, 2018a.

616 Suriya Gunasekar, Jason D Lee, Daniel Soudry, and Nati Srebro. Implicit bias of gradient descent on
 617 linear convolutional networks. *Advances in neural information processing systems*, 31, 2018b.

618 Tzu-Ming Harry Hsu, Hang Qi, and Matthew Brown. Measuring the effects of non-identical data
 619 distribution for federated visual classification. *arXiv preprint arXiv:1909.06335*, 2019.

620 Baihe Huang, Xiaoxiao Li, Zhao Song, and Xin Yang. Fl-ntk: A neural tangent kernel-based framework
 621 for federated learning analysis. In *International Conference on Machine Learning*, pp. 4423–4434.
 622 PMLR, 2021.

623 Yanping Huang, Youlong Cheng, Ankur Bapna, Orhan Firat, Dehao Chen, Mia Chen, HyoukJoong Lee,
 624 Jiquan Ngiam, Quoc V Le, Yonghui Wu, et al. Gpipe: Efficient training of giant neural networks using
 625 pipeline parallelism. *Advances in neural information processing systems*, 32, 2019.

626 Sami Jaghouar, Jack Min Ong, and Johannes Hagemann. Opendiloco: An open-source framework for
 627 globally distributed low-communication training. *arXiv preprint arXiv:2407.07852*, 2024.

628 Divyansh Jhunjhunwala, Shiqiang Wang, and Gauri Joshi. Fedexp: Speeding up federated averaging via
 629 extrapolation. In *The Eleventh International Conference on Learning Representations*, 2023.

630 Ziwei Ji and Matus Telgarsky. The implicit bias of gradient descent on nonseparable data. In *Conference
 631 on Learning Theory*, pp. 1772–1798. PMLR, 2019a.

632 Ziwei Ji and Matus Telgarsky. Gradient descent aligns the layers of deep linear networks. In *International
 633 Conference on Learning Representations*, 2019b.

634 Haoming Jiang, Pengcheng He, Weizhu Chen, Xiaodong Liu, Jianfeng Gao, and Tuo Zhao. Smart:
 635 Robust and efficient fine-tuning for pre-trained natural language models through principled regularized
 636 optimization. In *Proceedings of the 58th Annual Meeting of the Association for Computational
 637 Linguistics*, pp. 2177–2190, 2020.

638 Hyunji Jung, Hanseul Cho, and Chulhee Yun. Convergence and implicit bias of gradient descent on contin-
 639 ual linear classification. In *The Thirteenth International Conference on Learning Representations*, 2025.

648 Peter Kairouz, H Brendan McMahan, Brendan Avent, Aurélien Bellet, Mehdi Bennis, Arjun Nitin Bhagoji,
 649 Kallista Bonawitz, Zachary Charles, Graham Cormode, Rachel Cummings, et al. Advances and open
 650 problems in federated learning. *arXiv preprint arXiv:1912.04977*, 2019.

651

652 Sai Praneeth Karimireddy, Satyen Kale, Mehryar Mohri, Sashank Reddi, Sebastian Stich, and
 653 Ananda Theertha Suresh. Scaffold: Stochastic controlled averaging for federated learning. In
 654 *International Conference on Machine Learning*, pp. 5132–5143. PMLR, 2020.

655 Ahmed Khaled, Konstantin Mishchenko, and Peter Richtárik. Tighter theory for local sgd on identical and
 656 heterogeneous data. In *International Conference on Artificial Intelligence and Statistics*, pp. 4519–4529.
 657 PMLR, 2020.

658

659 Anastasia Koloskova, Nicolas Loizou, Sadra Boreiri, Martin Jaggi, and Sebastian Stich. A unified
 660 theory of decentralized SGD with changing topology and local updates. In Hal Daumé III and
 661 Aarti Singh (eds.), *Proceedings of the 37th International Conference on Machine Learning*, volume
 662 119 of *Proceedings of Machine Learning Research*, pp. 5381–5393. PMLR, 13–18 Jul 2020. URL
 663 <https://proceedings.mlr.press/v119/koloskova20a.html>.

664 Jakub Konečný, H Brendan McMahan, Felix X Yu, Peter Richtárik, Ananda Theertha Suresh, and
 665 Dave Bacon. Federated learning: Strategies for improving communication efficiency. *arXiv preprint*
 666 *arXiv:1610.05492*, 2016.

667 Simon Kornblith, Jonathon Shlens, and Quoc V Le. Do better imagenet models transfer better? In *Proceed-
 668 ings of the IEEE/CVF conference on computer vision and pattern recognition*, pp. 2661–2671, 2019.

669

670 Yiwen Kou, Zixiang Chen, and Quanquan Gu. Implicit bias of gradient descent for two-layer relu and leaky
 671 relu networks on nearly-orthogonal data. *Advances in Neural Information Processing Systems*, 36, 2024.

672 Tian Li, Anit Kumar Sahu, Manzil Zaheer, Mazyar Sanjabi, Ameet Talwalkar, and Virginia Smith.
 673 Federated optimization in heterogeneous networks. *Proceedings of Machine learning and systems*,
 674 2:429–450, 2020a.

675

676 Tian Li, Shengyuan Hu, Ahmad Beirami, and Virginia Smith. Ditto: Fair and robust federated learning
 677 through personalization. In *International Conference on Machine Learning*, pp. 6357–6368. PMLR,
 678 2021.

679 Xiang Li, Kaixuan Huang, Wenhao Yang, Shusen Wang, and Zhihua Zhang. On the convergence of
 680 FedAvg on non-IID data. In *International Conference on Learning Representations*, 2020b.

681

682 Sen Lin, Peizhong Ju, Yingbin Liang, and Ness Shroff. Theory on forgetting and generalization of
 683 continual learning. In *International Conference on Machine Learning*, pp. 21078–21100. PMLR, 2023.

684 Tao Lin, Sebastian U Stich, Kumar Kshitij Patel, and Martin Jaggi. Don't use large mini-batches, use
 685 local SGD. In *International Conference on Learning Representations*, 2019.

686

687 Shruti P Maralappanavar, Prashant Khanduri, and Bharath B N. Linear convergence of decentralized
 688 fedavg for PL objectives: The interpolation regime. *Transactions on Machine Learning Research*, 2025.
 689 ISSN 2835-8856. URL <https://openreview.net/forum?id=Og3VxBFhwj>.

690 Brendan McMahan, Eider Moore, Daniel Ramage, Seth Hampson, and Blaise Aguera y Arcas.
 691 Communication-efficient learning of deep networks from decentralized data. In *Artificial intelligence
 692 and statistics*, pp. 1273–1282. PMLR, 2017.

693

694 Mor Shpigel Nacson, Nathan Srebro, and Daniel Soudry. Stochastic gradient descent on separable data:
 695 Exact convergence with a fixed learning rate. In *The 22nd International Conference on Artificial
 696 Intelligence and Statistics*, pp. 3051–3059. PMLR, 2019.

697 Kumar Kshitij Patel, Margalit Glasgow, Ali Zindari, Lingxiao Wang, Sebastian U Stich, Ziheng
 698 Cheng, Nirmit Joshi, and Nathan Srebro. The limits and potentials of local sgd for distributed
 699 heterogeneous learning with intermittent communication. In Shipra Agrawal and Aaron Roth
 700 (eds.), *Proceedings of Thirty Seventh Conference on Learning Theory*, volume 247 of *Pro-
 701 ceedings of Machine Learning Research*, pp. 4115–4157. PMLR, 30 Jun–03 Jul 2024. URL
<https://proceedings.mlr.press/v247/patel124a.html>.

702 Tiancheng Qin, S Rasoul Etesami, and César A Uribe. Faster convergence of local sgd for
 703 over-parameterized models. *arXiv preprint arXiv:2201.12719*, 2022.

704

705 Sashank J Reddi, Zachary Charles, Manzil Zaheer, Zachary Garrett, Keith Rush, Jakub Konečný, Sanjiv
 706 Kumar, and Hugh Brendan McMahan. Adaptive federated optimization. In *International Conference
 707 on Learning Representations*, 2021.

708 Hamza Reguieg, Mohammed El Hanjri, Mohamed El Kamili, and Abdellatif Kobbane. A comparative
 709 evaluation of fedavg and per-fedavg algorithms for dirichlet distributed heterogeneous data. In *2023
 710 10th International Conference on Wireless Networks and Mobile Communications (WINCOM)*, pp.
 711 1–6. IEEE, 2023.

712 Alexander Sergeev and Mike Del Balso. Horovod: fast and easy distributed deep learning in tensorflow.
 713 *arXiv preprint arXiv:1802.05799*, 2018.

714

715 Bingqing Song, Prashant Khanduri, Xinwei Zhang, Jinfeng Yi, and Mingyi Hong. Fedavg converges
 716 to zero training loss linearly for overparameterized multi-layer neural networks. In *International
 717 Conference on Machine Learning*, pp. 32304–32330. PMLR, 2023.

718 Daniel Soudry, Elad Hoffer, Mor Shpigel Nacson, Suriya Gunasekar, and Nathan Srebro. The implicit bias
 719 of gradient descent on separable data. *The Journal of Machine Learning Research*, 19(1):2822–2878,
 720 2018.

721

722 Sebastian U Stich. Local SGD converges fast and communicates little. In *International Conference on
 723 Learning Representations*, 2019.

724

725 Canh T Dinh, Nguyen Tran, and Josh Nguyen. Personalized federated learning with moreau envelopes.
 726 *Advances in Neural Information Processing Systems*, 33:21394–21405, 2020.

727

728 Jianyu Wang, Qinghua Liu, Hao Liang, Gauri Joshi, and H Vincent Poor. Tackling the objective
 729 inconsistency problem in heterogeneous federated optimization. *Advances in neural information
 730 processing systems*, 33:7611–7623, 2020.

731

732 Jianyu Wang, Rudrajit Das, Gauri Joshi, Satyen Kale, Zheng Xu, and Tong Zhang. On the unreasonable
 733 effectiveness of federated averaging with heterogeneous data. *Transactions on Machine Learning
 734 Research*, 2024.

735

736 Blake Woodworth, Kumar Kshitij Patel, Sebastian Stich, Zhen Dai, Brian Bullins, Brendan McMahan,
 737 Ohad Shamir, and Nathan Srebro. Is local SGD better than minibatch SGD? In Hal Daumé III and
 738 Aarti Singh (eds.), *Proceedings of the 37th International Conference on Machine Learning*, volume
 739 119 of *Proceedings of Machine Learning Research*, pp. 10334–10343. PMLR, 13–18 Jul 2020. URL
 740 <https://proceedings.mlr.press/v119/woodworth20a.html>.

741

742 Shuo Xie and Zhiyuan Li. Implicit bias of adamw: ℓ_∞ -norm constrained optimization. In *International
 743 Conference on Machine Learning*, pp. 54488–54510. PMLR, 2024.

744

745 Hao Yu, Sen Yang, and Shenghuo Zhu. Parallel restarted sgd with faster convergence and less
 746 communication: Demystifying why model averaging works for deep learning. In *Proceedings of the
 747 AAAI conference on artificial intelligence*, pp. 5693–5700, 2019.

748

749 Chenyang Zhang, Difan Zou, and Yuan Cao. The implicit bias of adam on separable data. *Advances
 750 in Neural Information Processing Systems*, 37:23988–24021, 2024.

751

752

753

754

755

756	CONTENTS	
757		
758		
759	1 Introduction	1
760	1.1 Related Work	2
761		
762	2 Motivating Observation in Linear Regression	4
763		
764		
765	3 Implicit Bias of Local-GD for Classification	4
766	3.1 Setting	4
767	3.2 Loss Convergence and Implicit Bias of Local-GD	5
768		
769	3.3 Discussions	6
770		
771	4 Implicit Bias of Local-GD with Learning Rate Independent of L	7
772	4.1 Setting	7
773	4.2 Implicit Bias of Local-GD and Relation to PPM	7
774		
775	4.3 Convergence to Global Feasible Set	8
776		
777	4.4 Modified Local-GD: Convergence to Centralized Model	8
778		
779	5 Experiments	9
780	5.1 Linear Classification	9
781	5.2 Fine-Tuning of Pretrained Neural Network	10
782		
783		
784	6 Conclusions	10
785		
786		
787	A Additional Experiments	17
788	A.1 Experiments on Linear Regression	17
789	A.2 Linear Classification with Dirichlet Distribution	17
790		
791		
792	B Local-GD for Linear Regression in Overparameterized Regime	18
793	B.1 Setting	18
794	B.2 Implicit Bias of Local GD in Linear Regression	18
795		
796	B.3 Convergence to Centralized Model	19
797		
798	B.4 Proofs in Linear Regression	20
799	B.4.1 Proof of Lemma 4	20
800	B.4.2 Proof of Theorem 1	21
801		
802		
803	C Proofs of Implicit Bias for Linear Classification in Section 3	23
804	C.1 Proof of Claim 1	23
805	C.1.1 Proof of Lemma 6	25
806		
807	C.2 Proof of Claim 2	27
808	C.2.1 Proof of Lemma 8	30
809		
	C.3 Proof of Claim 3	30

810	D Proofs of Implicit Bias with Learning Rate Independent of L in Section 4	32
811	D.1 Proofs of Lemma 1	32
812	D.2 Proofs of Auxiliary Lemmas	34
813	D.3 Lemma and Proofs in Section 4.4	37
814		
815		
816		
817		
818		
819		
820		
821		
822		
823		
824		
825		
826		
827		
828		
829		
830		
831		
832		
833		
834		
835		
836		
837		
838		
839		
840		
841		
842		
843		
844		
845		
846		
847		
848		
849		
850		
851		
852		
853		
854		
855		
856		
857		
858		
859		
860		
861		
862		
863		

864

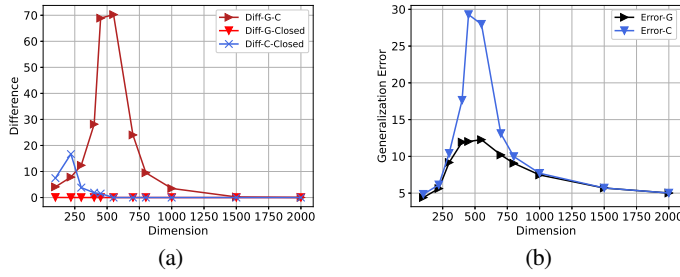
A ADDITIONAL EXPERIMENTS

865

A.1 EXPERIMENTS ON LINEAR REGRESSION

866 We simulated 10 compute nodes, each with 50 training samples. The label vector y_i at i -th compute node
 867 is exactly generated as (13), where ground truth model w_i^* is Gaussian vector with each element following
 868 $\mathcal{N}(0,4)$. Each ground truth model at different compute nodes is independently generated, thus the datasets
 869 can be very different from each other. The data matrix X_i also follows Gaussian distribution, with each
 870 element being $\mathcal{N}(0,1)$, and z_i is a Gaussian vector with $\mathcal{N}(0,0.04)$. In Local-GD, the number of local
 871 steps is $L=200$, number of rounds is also $R=200$, and the learning rate $\eta=0.0001$. Actually it just take
 872 a few local steps to converge locally at each round, but we set a large number of local steps to show it
 873 can be large at $O(\sqrt{T})$, where $T=L \cdot R$ is the number of total iterations. We tested the global model
 874 (G) from Local-GD on squared loss, centralized model (C) trained from global dataset on squared loss,
 875 closed form of global model (G-Closed) in (17), closed form of centralized model (C-Closed) as solution
 876 of problem (18). The centralized model is trained 10000 steps with learning rate 0.0001.
 877

878 Fig. 2(a) displays the difference between global model and centralized model, global model and its closed
 879 form, and centralized model and its closed form, with respect to model dimension. The difference between
 880 two models is $\|w_1 - w_2\|/d$. Since it is always locally overparameterized, the difference between global
 881 model and the closed form is always zero. The difference between global model and centralized model
 882 has an obvious peak around 500, which is the number of total samples. The phenomenon that global model
 883 converges exactly to centralized model only happens when the model is sufficiently overparameterized.
 884 Fig. 2(b) shows the generalization error of global model and centralized model in linear regression. Since
 885 the data matrix is Gaussian, the generalization error of model w can be computed as $\frac{1}{M} \sum_{i=1}^M \|w - w_i^*\|^2$.
 886 We plot the generalization error divided by d . It is shown the global model and centralized model can
 887 get the same performance when model is sufficiently overparameterized.
 888



900 Figure 2: (a) Difference between global and centralized models plotted against increasing dimension. (b)
 901 Generalization error with respect to dimension.

902

A.2 LINEAR CLASSIFICATION WITH DIRICHLET DISTRIBUTION

903 In federated learning, the Dirichlet distribution is usually used to generate heterogeneous datasets across the
 904 compute nodes Hsu et al. (2019); Chen & Chao (2021); Reguieg et al. (2023). For binary classification prob-
 905 lem, the Dirichlet distribution $\text{Dir}(\alpha)$ is used to unbalance the positive and negative samples. In the exper-
 906 iments we have 10 compute nodes. We generate 500 samples as $y_i = \text{sign}(x_i^T w^*)$ for $i \in [500]$ and use $\text{Dir}(\alpha)$
 907 to distribute the 500 samples across 10 compute nodes. Note that the number of samples at each compute
 908 node is not necessarily identical. Fig. 3 shows performance of Local-GD for linear classification with differ-
 909 ent parameter α in Dirichlet distribution. The λ is set to be 0.0001 and model dimension is fixed as $d=1500$.
 910 The number of local steps L is 150 and number of communication rounds R is 150. The learning rate is 0.01.
 911 The centralized model is trained with the same learning rate for 22500 steps. We can see the global model
 912 and modified global model still converge to the centralized model in direction and get similar test accuracy.
 913

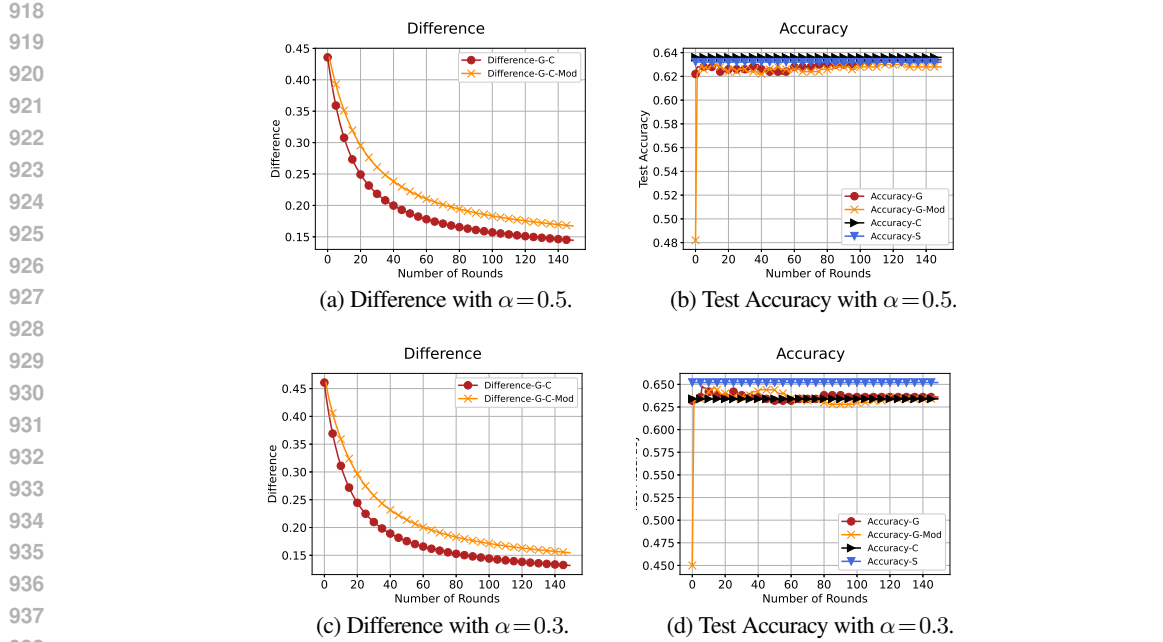


Figure 3: Local-GD on linear classification with Dirichlet distribution.

B LOCAL-GD FOR LINEAR REGRESSION IN OVERPARAMETERIZED REGIME

In this section we give a extended description of Section 2 about linear regression in overparameterized regime.

B.1 SETTING

The behavior of linear regression is very well-understood in high-dimensional statistics; and we can clearly convey our key message based on this fundamental setting.

At each compute node i , the dataset S_i consists of N tuples of samples and their corresponding labels, $(x, y) \in \mathbb{R}^d \times \mathbb{R}$. We assume the label y_{ij} is generated by

$$y_{ij} = x_{ij}^T w_i^* + z_{ij} \quad (13)$$

where $w_i^* \in \mathbb{R}^d$ is the ground truth model at i -th compute node, and z_{ij} is the added noise. Denote $X_i = [x_{i1}, x_{i2}, \dots, x_{iN}]^T \in \mathbb{R}^{N \times d}$ as the data matrix at i -th compute node, and $y_i = [y_{i1}, y_{i2}, \dots, y_{iN}] \in \mathbb{R}^N$ as the label vector, $z_i \in \mathbb{R}^N$ as the noise vector. In heterogeneous setting, the w_i^* can be very different to each other. Note that the convergence to centralized model does not rely on the generative model. We just make this assumption on generative model for deriving a more clear form of the aggregated global model.

Algorithm. At each round, the aggregator sends the global model w_0 to all the compute nodes. Each compute node minimizes the squared loss $f_i(w_i) = \frac{1}{2N} \|y_i - X_i w_i\|^2$ by a large number of gradient descent steps *until convergence*. Then each compute node sends back the local model and the aggregator aggregates all the local models to get the updated global model. The detailed algorithm is Local-GD in Algorithm 1 with $f_i(w_i)$ replaced in the update. Since minimizing squared loss is a quadratic problem, it is expected to reach convergence locally with a small number of gradient descent steps.

B.2 IMPLICIT BIAS OF LOCAL GD IN LINEAR REGRESSION

For each local problem, when the dimension of the model is larger than the number of samples at each compute node ($d > N$), i.e., locally overparameterized, there are multiple solutions corresponding to zero squared loss. However, gradient descent will lead the model converge to a specific solution, which corresponds to a minimum Euclidean distance to the initial point Gunasekar et al. (2018a); Evron et al. (2022). Formally, the

972 solution w_i^{k+1} obtained at k -th round and i -th node will converge to the solution of the optimization problem
 973

$$974 \quad \min_{w_i} \|w_i - w_0^k\|^2 \quad \text{s.t.} \quad X_i w_i = y_i. \quad (14)$$

975

976 We can obtain the closed form solution of this optimization problem as (see Proof of Lemma 4 in
 977 Appendix B.4.1)

$$978 \quad w_i^{k+1} = (I - X_i^T (X_i X_i^T)^{-1} X_i) w_0^k + X_i^T (X_i X_i^T)^{-1} y_i \\ 979 \quad = (I - X_i^T (X_i X_i^T)^{-1} X_i) w_0^k \\ 980 \quad + X_i^T (X_i X_i^T)^{-1} X_i w_i^* + X_i^T (X_i X_i^T)^{-1} z_i. \quad (15)$$

981

982 Denote $P_i \triangleq X_i^T (X_i X_i^T)^{-1} X_i$ and $X_i^\dagger \triangleq X_i^T (X_i X_i^T)^{-1}$. The local model can be rewritten as
 983 $w_i^{k+1} = (I - P_i) w_0^k + P_i w_i^* + X_i^\dagger z_i$. We observe that P_i is the projection operator to the row space of
 984 X_i , and X_i^\dagger is the pseudo inverse of X_i . After one round of iterations, the local model is actually an
 985 interpolation between the initial global model w_0^k at this round and the ground-truth model w_i^* , plus
 986 a noise term. We then obtain the closed form of global model by aggregation. After many rounds of
 987 communication, we can obtain the final trained global model from Local-GD.

988 **Lemma 4.** *When the local overparameterized linear regression problems are exactly solved by gradient
 989 descent, then after K rounds of communication, the global model w_0^K obtained from Local-GD is*

$$990 \quad w_0^K = (I - \bar{P})^K w_0^0 + \sum_{k=0}^{K-1} (I - \bar{P})^k (\bar{Q} + \bar{Z}), \quad (16)$$

991

992 where $\bar{P} = \frac{1}{M} \sum_{i=1}^M P_i$, $\bar{Q} = \frac{1}{M} \sum_{i=1}^M P_i w_i^*$, $\bar{Z} = \frac{1}{M} \sum_{i=1}^M X_i^\dagger z_i$.

993 Note that $\bar{P}, \bar{Q}, \bar{Z}$ are constant after the data is generated. Since we only know the $\{X_i, y_i\}_{i=1}^M$ in the
 994 training process, we can also write it as

$$995 \quad w_0^K = (I - \bar{P})^K w_0^0 + \sum_{k=0}^{K-1} (I - \bar{P})^k \bar{Y}, \quad (17)$$

996

997 where $\bar{Y} = \frac{1}{M} \sum_{i=1}^M X_i^\dagger y_i$. Then we can directly get the final model from the training set.

998 **Singularity of \bar{P} .** If \bar{P} is invertible, we can further simplify the form of global model. However, since
 999 $P_i \in \mathbb{R}^{d \times d}$ is the projection operator onto row space of X_i , its rank is at most N . The \bar{P} is the average
 1000 of P_i s, thus its rank is at most MN . Note that we consider the overparameterized regime both locally
 1001 and globally, i.e., $d \gg MN$. Then \bar{P} is singular, and the sum $\sum_{k=0}^{K-1} (I - \bar{P})^k$ approaches KI when
 1002 d becomes very large. We cannot get more properties of the final global model from (17), but we can
 1003 compare it to the centralized model trained with all of the data.

1004 B.3 CONVERGENCE TO CENTRALIZED MODEL

1005 Let $X_c = [X_1^T, \dots, X_M^T]^T \in \mathbb{R}^{MN \times d}$ be the data matrix consisting of all the local data, and
 1006 $y_c = [y_1^T, \dots, y_M^T]^T \in \mathbb{R}^{MN \times 1}$ be the label vector consisting of the local labels. If we train the centralized
 1007 model from initial point 0 with squared loss, then the gradient descent will lead the model to the solution
 1008 of the optimization problem

$$1009 \quad \min_w \|w\|^2 \quad \text{s.t.} \quad X_c w = y_c \quad (18)$$

1010

1011 We can write the closed form of centralized model as $w_c = X_c^T (X_c X_c^T)^{-1} y_c$.

1012 Due to the constraint in problem (18), for each compute node i , we have $X_i w_c = y_i$. We replace y_i in
 1013 the local model (15), then we have

$$1014 \quad w_i^{k+1} - w_c = (I - P_i)(w_0^k - w_c). \quad (19)$$

1015

1016 The RHS is projecting the difference between global model and centralized model onto null space of X_i .
 1017 After averaging all the local models at the aggregator, we have

$$1018 \quad w_0^{k+1} - w_c = (I - \bar{P})(w_0^k - w_c). \quad (20)$$

1019

1026 In the training process the difference between global model and centralized model is iteratively projected
 1027 onto the null space of span of row spaces of X_i s. It implies that the difference on the span of data matrix
 1028 gradually decreases until zero. Based on the evolution of the difference, we can prove the Theorem 1
 1029 and we restate it here:

1030 **Theorem 5.** *For the linear regression problem, suppose the initial point w_0^0 is 0 and $d > MN$ and
 1031 the minimum eigenvalue of \bar{P} , λ_{\min} is larger than 0, then the global model obtained by Local-GD,
 1032 w_0^K , converges to the centralized solution w_c as the number of communication rounds $K \rightarrow \infty$ as
 1033 $\|w_0^K - w_c\| \leq (1 - \lambda_{\min})^K \|w_c\|$.*

1034 The proof is in Appendix B.4.2. The key step is to show the initial difference is already in the data space,
 1035 and no residual in the null space of row spaces of X_i s. The convergence to the centralized model is at
 1036 exponential rate.

1037 Due to the linearity of the regression problem, we can theoretically show the global model can exactly
 1038 converge to the centralized model with implicit bias on overparameterized regime. Note that the proof
 1039 does not rely on the generative model and assumption on data heterogeneity. It implies that, even if we
 1040 use a large number of local steps to exactly solve the local problems on very heterogeneous data, the
 1041 performance of Local-GD is equivalent to train a model with all the data in one place.

1043 B.4 PROOFS IN LINEAR REGRESSION

1044 B.4.1 PROOF OF LEMMA 4

1045 At each compute node, the local model converges to the solution of problem

$$1046 \min_{w_i} \|w_i - w_0^k\|^2 \quad \text{s.t.} \quad X_i w_i = y_i. \quad (21)$$

1047 Using Lagrange multipliers, we can write the Lagrangian as

$$1048 \frac{1}{2} \|w_i - w_0^k\|^2 + \beta^T (X_i w_i - y_i) \quad (22)$$

1049 Setting the derivative to 0, we know the optimal \tilde{w}_i satisfies

$$1050 \tilde{w}_i - w_0^k + X_i^T \beta = 0, \quad (23)$$

1051 and then

$$1052 \tilde{w}_i = w_0^k - X_i^T \beta. \quad (24)$$

1053 Also by the constraint $y_i = X_i \tilde{w}_i$, we can get

$$1054 y_i = X_i w_0^k - (X_i X_i^T) \beta. \quad (25)$$

1055 Since the model is overparameterized ($d > N$), $X_i X_i^T \in \mathbb{R}^{d \times d}$ is invertible. Then we have

$$1056 \beta = -(X_i X_i^T)^{-1} (y_i - X_i w_0^k). \quad (26)$$

1057 Plugging the β back, we can get the closed form solution as

$$1058 \tilde{w}_i = w_0^k + X_i^T (X_i X_i^T)^{-1} (y_i - X_i w_0^k). \quad (27)$$

1059 We update the local model $w_i^{k+1} = \tilde{w}_i$.

1060 We can also write the closed form solution as

$$1061 \begin{aligned} w_i^{k+1} &= w_0^k + X_i^T (X_i X_i^T)^{-1} (y_i - X_i w_0^k) \\ 1062 &= (I - X_i^T (X_i X_i^T)^{-1} X_i) w_0^k + X_i^T (X_i X_i^T)^{-1} y_i \end{aligned} \quad (28)$$

1063 If we plug in the generative model $y_i = X_i w_i^* + z_i$, then the solution is

$$1064 \begin{aligned} w_i^{k+1} &= (I - X_i^T (X_i X_i^T)^{-1} X_i) w_0^k + X_i^T (X_i X_i^T)^{-1} X_i w_i^* + X_i^T (X_i X_i^T)^{-1} z_i \\ 1065 &= (I - P_i) w_0^k + P_i w_i^* + X_i^T z_i. \end{aligned} \quad (29)$$

1080 where $P_i = X_i^T (X_i X_i^T)^{-1} X_i$ is the projection operator to the row space of X_i , and $X_i^\dagger = X_i^T (X_i X_i^T)^{-1}$
 1081 is the pseudo inverse of X_i . It is an interpolation between the initial global model w_0^k and the local true
 1082 model w_i^* , plus a noise term.
 1083

1084 After aggregating all the local models, the global model is

$$\begin{aligned} 1085 \quad w_0^{k+1} &= \frac{1}{m} \sum_{i=1}^m (I - P_i) w_0^k + \frac{1}{m} \sum_{i=1}^m P_i w_i^* + \frac{1}{m} \sum_{i=1}^m X_i^\dagger z_i \\ 1086 \quad &= (I - \bar{P}) w_0^k + \bar{Q} + \bar{Z}, \end{aligned} \quad (30)$$

1089 where $\bar{P} = \frac{1}{m} \sum_{i=1}^m P_i$, $\bar{Q} = \sum_{i=1}^m P_i w_i^*$, $\bar{Z} = \frac{1}{m} \sum_{i=1}^m X_i^\dagger z_i$.

1090 After K rounds of communication, the global model is
 1091

$$1093 \quad w_0^K = (I - \bar{P})^K w_0^0 + \sum_{k=0}^{K-1} (I - \bar{P})(\bar{Q} + \bar{Z}). \quad (31)$$

1096 If we start from $w_0^0 = 0$, then the solution will converge to $\sum_{k=0}^{K-1} (I - \bar{P})(\bar{Q} + \bar{Z})$.
 1097

1098 B.4.2 PROOF OF THEOREM 1

1100 We know the difference between global model and centralized model is iteratively projected onto the null
 1101 space of span of row spaces of X_i s:

$$1102 \quad w_0^{k+1} - w_c = (I - \bar{P})(w_0^k - w_c). \quad (32)$$

1104 We can formally describe it as follows. Since the problem is overparameterized globally, we can assume
 1105 each X_i has full rank N . We apply singular value decomposition (SVD) to X_i as $X_i = U_i \Sigma_i V_i^T$, where
 1106 $U_i \in \mathbb{R}^{N \times N}$, $V_i \in \mathbb{R}^{d \times N}$. Then $P_i = X_i^T (X_i X_i^T)^{-1} X_i = V_i V_i^T$, which is the projection matrix to the row
 1107 space of X_i .
 1108

1109 We apply eigenvalue decomposition on \bar{P} to get $\bar{P} = Q \Sigma Q^T$, where $Q \in \mathbb{R}^{d \times n'}$ and n' is the rank of \bar{P} .
 1110 It satisfies $N \leq n' \leq MN$. Since \bar{P} is a linear combination of P_i s, the space of column space of Q is
 1111 the space spanned by all the vectors $v_{ij}, i=1, \dots, M, j=1, \dots, N$.

1112 We also construct a matrix $Q' \in \mathbb{R}^{d \times (d-n')}$, which consists of orthonormal vectors perpendicular to Q .
 1113 We can project the difference onto column space of Q and Q' respectively.
 1114

$$\begin{aligned} 1115 \quad Q^T(w_0^{k+1} - w_c) &= Q^T(I - Q \Sigma Q^T)(w_0^k - w_c) = (I - \Sigma)Q^T(w_0^k - w_c) \\ 1116 \quad Q'^T(w_0^{k+1} - w_c) &= Q'^T(I - Q \Sigma Q^T)(w_0^k - w_c) = Q'^T(w_0^k - w_c) \end{aligned} \quad (33)$$

1118 After K rounds of communication, we can decompose $w_0^K - w_c$ into two parts:
 1119

$$1120 \quad w_0^K - w_c = Q Q^T(w_0^K - w_c) + Q' Q'^T(w_0^K - w_c). \quad (34)$$

1122 Then we can obtain

$$\begin{aligned} 1123 \quad w_0^K - w_c &= Q Q^T(w_0^K - w_c) + Q' Q'^T(w_0^K - w_c) \\ 1124 \quad &= Q(I - \Sigma)^K Q^T(w_0^0 - w_c) + Q' Q'^T(w_0^0 - w_c). \end{aligned}$$

1126 It shows the initial difference on the column space of Q continues to decrease until zero if K is sufficiently
 1127 large. And the initial difference on the null space of Q remains constant.

1128 To show the difference $w_0^K - w_c$ goes to zero entirely, we just need to choose an initial point such that
 1129 initial difference is on the column space of Q . When we choose $w_0^0 = 0$, the initial difference is w_c itself.
 1130 Moreover, the centralized solution $w_c = X_c^T (X_c X_c^T)^{-1} y_c$ exactly lies in the data space spanned by vectors
 1131 $\{v_{ij}\}_{i=1, j=1}^{M, N}$ since it is a linear combination of columns of X_c^T . So if we start from $w_0^0 = 0$, then $w_0^K - w_c$
 1132 will go to zero when K is sufficiently large.
 1133

When starting from 0, the difference between the global model and the centralized model becomes

1134

1135

$$\begin{aligned}
 \|w_0^K - w_c\|^2 &= \|Q(I - \Sigma)^K Q^T w_c\|^2 \\
 &= (Q(I - \Sigma)^K Q^T w_c)^T (Q(I - \Sigma)^K Q^T w_c) \\
 &= (Q^T w_c)^T (I - \Sigma)^{2K} (Q^T w_c).
 \end{aligned} \tag{35}$$

1140

1141 Since $I - \Sigma$ is a diagonal matrix, we can get

1142 $\|w_0^K - w_c\|^2 \leq (1 - \lambda_{\min})^{2K} \|Q^T w_c\|^2,$ 1143

1144 where λ_{\min} is the minimum eigenvalue of matrix \bar{P} . Also since Q is an orthogonal matrix, we have
1145 $\|Q^T w_c\|^2 = \|w_c\|^2$. Then we can get

1146 $\|w_0^K - w_c\| \leq (1 - \lambda_{\min})^K \|w_c\|.$ 1147

1148

1149 It shows the difference between trained global model and centralized model converge to zero at an
1150 exponential rate.

1151

1152

1153

1154

1155

1156

1157

1158

1159

1160

1161

1162

1163

1164

1165

1166

1167

1168

1169

1170

1171

1172

1173

1174

1175

1176

1177

1178

1179

1180

1181

1182

1183

1184

1185

1186

1187

1188 **C PROOFS OF IMPLICIT BIAS FOR LINEAR CLASSIFICATION IN SECTION 3**
 1189

1190 We give the detailed proofs of Theorem 2 in this section. The proof framework is inspired by the analysis
 1191 of implicit bias of SGD Nacson et al. (2019). Intuitively, we can regard one local dataset as a “batch” in
 1192 SGD for sampling without replacement. But we perform multiple gradient steps in the same “batch”, not
 1193 just one step of gradient descent. The challenge is to handle local steps in the same local dataset and the
 1194 aggregation after one round of local training. Here we restate the Theorem 2.

1195 **Theorem 6.** *Under assumptions 1, 2, 3, if the learning rate satisfies $\eta \leq \min\left(\frac{1}{2L\sigma_{\max}^2\beta}, \frac{\gamma^2}{4L\sigma_{\max}^3\beta(\gamma+\sigma_{\max})}\right)$,
 1196 then for the process of Local-GD, we have,*

1197

- **Claim 1:** Every data point is classified correctly finally: $\lim_{k \rightarrow \infty} x_s^T w_0^k = \infty, \forall s \in S$.
- **Claim 2:** The global model obtained from Local-GD will behave as

1202
$$w_0^k = \log(Lk)\hat{w} + \rho^k, \quad \text{and,} \quad \left\| \frac{w_0^k}{\|w_0^k\|} - \frac{\hat{w}}{\|\hat{w}\|} \right\| = O\left(\frac{1}{\log Lk}\right) \quad (38)$$

1204 and $\|\rho^k\| < \infty$ for all k . This implies, the normalized global model converges to the global
 1205 max-margin solution.

1206

- **Claim 3:** The loss function $f(w_0^k)$ decreases to zero as $f(w_0^k) = O\left(\frac{1}{Lk}\right)$.

1208 For the three claims in Theorem 2, we will give separable (but sequential) proofs below. In the proofs of
 1209 linear classification, for ease of notation, we redefine the samples $y_s x_s$ to x_s to subsume the labels.

1211 **C.1 PROOF OF CLAIM 1**
 1212

1213 In this proof, we rely on the key property of linearly separable data.

1214 **Lemma 5** (Lemma 2 and (17) in Nacson et al. (2019)). *Suppose that Assumptions 1 and 2 hold. For
 1215 any $w \in \mathbb{R}^d$,*

1217
$$\|\nabla f(w)\| \geq \frac{\gamma}{M} \sqrt{\sum_{s \in S} [g'(x_s^T w)]^2}.$$

1219 **Lemma 6.** *Suppose that Assumptions 1 and 2 hold and $k \in \mathbb{N}$. Then we have*

1221
$$\|w_i^{k,l} - w_0^k + \eta(l\nabla f_i(w_0^k))\| \leq \frac{\eta^2 L \sigma_{\max}^3 \beta M l}{\gamma(1 - l\eta\beta\sigma_{\max}^2)} \|\nabla f(w_0^k)\|. \quad (39)$$

1224
$$\|w_i^{k,l} - w_0^k\| \leq \frac{\eta L \sigma_{\max} M}{\gamma(1 - l\eta\beta\sigma_{\max}^2)} \|\nabla f(w_0^k)\|. \quad (40)$$

1228
$$\|\nabla f(w_i^{k,l}) - \nabla f(w_0^k)\| \leq \frac{\eta L \sigma_{\max}^3 \beta M}{\gamma(1 - l\eta\beta\sigma_{\max}^2)} \|\nabla f(w_0^k)\|. \quad (41)$$

1230 The proof can be seen in Section C.1.1.

1232 Note that $f(w) = \frac{1}{M} \sum_{i=1}^M f_i(w) = \frac{1}{M} \sum_{s \in S} g(x_s^T w)$, and $g(u)$ is a β -smooth function from Assumption
 1233 2. Then $f(w)$ is a $\frac{\beta\sigma_{\max}^2}{M}$ -smooth function. Then we can get

1235
$$\begin{aligned} & f(w_0^{k+1}) - f(w_0^k) - \frac{\sigma_{\max}^2 \beta}{2M} \|w_0^{k+1} - w_0^k\|^2 \\ & \leq \langle \nabla f(w_0^k), (w_0^{k+1} - w_0^k) \rangle \\ & = \langle \nabla f(w_0^k), w_0^{k+1} - w_0^k - \eta L \nabla f(w_0^k) + \eta L \nabla f(w_0^k) \rangle \\ & \leq -\eta L \|\nabla f(w_0^k)\|^2 + \|\nabla f(w_0^k)\| \|w_0^{k+1} - w_0^k + \eta L \nabla f(w_0^k)\|, \end{aligned} \quad (42)$$

1241 where the second inequality is from Cauchy-Schwarz inequality.

For the second term, we have

$$\begin{aligned}
& \|w_0^{k+1} - w_0^k + \eta L \nabla f(w_0^k)\| \\
&= \left\| \frac{1}{M} \sum_{i=1}^M w_i^{k+1} - w_0^k + \eta L \frac{1}{M} \sum_{i=1}^M \nabla f_i(w_0^k) \right\| \\
&\leq \frac{1}{M} \sum_{i=1}^M \|w_i^{k+1} - w_0^k + \eta L \nabla f_i(w_0^k)\| \\
&\leq \frac{1}{M} \sum_{i=1}^M \frac{\eta^2 L^2 \sigma_{\max}^3 \beta M}{\gamma(1 - L\eta\beta\sigma_{\max}^2)} \|\nabla f(w_0^k)\| \\
&= \frac{\eta^2 L^2 \sigma_{\max}^3 \beta M}{\gamma(1 - L\eta\beta\sigma_{\max}^2)} \|\nabla f(w_0^k)\|
\end{aligned} \tag{43}$$

where the first inequality is triangle inequality and second inequality is from Lemma 6.

We also have

$$\begin{aligned}
\|w_0^{k+1} - w_0^k\|^2 &= \left\| \frac{1}{M} \sum_{i=1}^M w_i^{k+1} - w_0^k \right\|^2 \\
&\leq \frac{1}{M} \sum_{i=1}^M \|w_i^{k+1} - w_0^k\|^2 \\
&\leq \frac{\eta^2 L^2 \sigma_{\max}^2 M^2}{\gamma^2 (1 - L\eta\beta\sigma_{\max}^2)^2} \|\nabla f(w_0^k)\|^2
\end{aligned} \tag{44}$$

where the second inequality is from Lemma 6. Plug above two inequalities into (42), we can get

$$f(w_0^{k+1}) - f(w_0^k) \leq -\eta L \left(1 - \frac{\eta L \sigma_{\max}^3 \beta M}{\gamma(1 - L\eta\beta\sigma_{\max}^2)} - \frac{\eta L \sigma_{\max}^4 \beta M}{2\gamma^2(1 - L\eta\beta\sigma_{\max}^2)^2} \right) \|\nabla f(w_0^k)\|^2 \quad (45)$$

If we choose $\eta \leq \frac{1}{2L\sigma_{\max}^2\beta}$, then $\frac{1}{1-L\eta\beta\sigma_{\max}^2} \leq 2$. Thus we can obtain

$$\begin{aligned} f(w_0^{k+1}) - f(w_0^k) &\leq -\eta L \left(1 - \eta L \sigma_{\max}^3 \beta M \left(\frac{2}{\gamma} + \frac{2\sigma_{\max}}{\gamma^2} \right) \right) \|\nabla f(w_0^k)\|^2 \\ &= -\eta L (1 - \eta L \beta') \|\nabla f(w_0^k)\|^2 \end{aligned} \quad (46)$$

where $\beta' = \frac{2\sigma_{\max}^3 \beta M(\gamma + \sigma_{\max})}{\gamma^2}$.

If we also choose $\eta \leq \frac{1}{2L\beta'}$, then

$$f(w_0^{k+1}) - f(w_0^k) \leq -\frac{\eta L}{2} \|\nabla f(w_0^k)\|^2, \quad (47)$$

which means the loss continues to decrease.

Combining the two condition on step size, we require

$$\eta \leq \min \left(\frac{1}{2L\sigma_{\max}^2\beta}, \frac{\gamma^2}{4L\sigma_{\max}^3\beta M(\gamma + \sigma_{\max})} \right). \quad (48)$$

Summing up from $k=0$ to ∞ we have

$$\sum_{k=0}^{\infty} \|\nabla f(w_0^k)\|^2 \leq \frac{2(f(w_0^0) - f(w_0^{\infty}))}{\eta L} \leq \frac{2f(w_0^0)}{\eta L} < \infty \quad (49)$$

The boundedness means $\lim_{k \rightarrow \infty} \|\nabla f(w_0^k)\|^2 = 0$. From Lemma 5, we can also know $\lim_{k \rightarrow \infty} g'(x_s^T w_0^k) = 0, \forall s \in S$. From Assumption 2, $g'(u) \rightarrow 0$ only when $u \rightarrow \infty$, thus $x_s^T w_0^k \rightarrow \infty, \forall s \in S$, which means all the training samples can be correctly classified. This proves Claim 1 in Theorem 2.

1296 We also bound the change of weights across iterations here, which is useful in the proof of Claim 2. since
 1297 $\nabla f_i(w) = \sum_{s \in S_i} g'(x_s^T w) x_s$ we can have
 1298

$$\begin{aligned}
 1300 \quad & \frac{1}{M} \sum_{i=1}^M \|w_i^{k,l+1} - w_i^{k,l}\| = \frac{1}{M} \sum_{i=1}^M \eta \|\nabla f_i(w_i^{k,l})\| \\
 1301 \quad & = \frac{1}{M} \sum_{i=1}^M \eta \left\| \sum_{s \in S_i} g'(x_s^T w_i^{k,l}) x_s \right\| \\
 1302 \quad & \leq \frac{1}{M} \sum_{i=1}^M \eta \sigma_{\max} \sqrt{\sum_{s \in S_i} (g'(x_s^T w_i^{k,l}))^2} \\
 1303 \quad & \leq \frac{1}{M} \sum_{i=1}^M \eta \sigma_{\max} \sqrt{\sum_{s \in S} (g'(x_s^T w_i^{k,l}))^2} \\
 1304 \quad & \leq \frac{\eta \sigma_{\max}}{\gamma} \sum_{i=1}^M \|\nabla f(w_i^{k,l})\|, \tag{50}
 \end{aligned}$$

1315 where the first inequality is from the fact $\|\sum_{s \in S} a_s x_s\| \leq \sigma_{\max} \sqrt{\sum_{s \in S} a_s^2}$ for $\forall a_s \in \mathbb{R}$, the second
 1316 inequality is due to $S_i \subset S$, and the final inequality is from Lemma 5. Further we can obtain
 1317

$$\begin{aligned}
 1319 \quad & \|\nabla f(w_i^{k,l})\| \leq \|\nabla f(w_0^k)\| + \|\nabla f(w_i^{k,l}) - \nabla f(w_0^k)\| \\
 1320 \quad & \leq \|\nabla f(w_0^k)\| + \frac{\eta L \sigma_{\max}^3 \beta M}{\gamma(1 - l\eta\beta\sigma_{\max}^2)} \|\nabla f(w_0^k)\| \\
 1321 \quad & = \left(1 + \frac{\eta L \sigma_{\max}^3 \beta M}{\gamma(1 - l\eta\beta\sigma_{\max}^2)}\right) \|\nabla f(w_0^k)\| \tag{51}
 \end{aligned}$$

1326 where the second inequality is from Lemma 6. Then we have

$$\begin{aligned}
 1329 \quad & \frac{1}{M} \sum_{i=1}^M \|w_i^{k,l+1} - w_i^{k,l}\|^2 \leq \frac{1}{M} \sum_{i=1}^M \frac{\eta^2 \sigma_{\max}^2 M^2}{\gamma^2} \left(1 + \frac{\eta L \sigma_{\max}^3 \beta M}{\gamma(1 - l\eta\beta\sigma_{\max}^2)}\right)^2 \|\nabla f(w_0^k)\|^2 \\
 1330 \quad & \leq \frac{\eta^2 \sigma_{\max}^2 M^2}{\gamma^2} \left(1 + \frac{\eta L \sigma_{\max}^3 \beta M}{\gamma(1 - l\eta\beta\sigma_{\max}^2)}\right)^2 \|\nabla f(w_0^k)\|^2 \tag{52}
 \end{aligned}$$

1336 Summing up all the changes, we can finally have

$$\frac{1}{M} \sum_{k=0}^{\infty} \sum_{l=1}^{L-1} \sum_{i=1}^M \|w_i^{k,l+1} - w_i^{k,l}\|^2 \leq \frac{\eta^2 \sigma_{\max}^2 L M^2}{\gamma^2} \left(1 + \frac{\eta L \sigma_{\max}^3 \beta M}{\gamma(1 - L\eta\beta\sigma_{\max}^2)}\right)^2 \sum_{k=0}^{\infty} \|\nabla f(w_0^k)\|^2 < \infty. \tag{53}$$

C.1.1 PROOF OF LEMMA 6

1345 *Proof.* We start from the update rule:

$$w_i^{k,l} = w_0^k - \eta \left(\sum_{l'=0}^{l-1} \nabla f_i(w_i^{k,l'}) \right). \tag{54}$$

1350 Define $\Delta := w_i^{k,l} - w_0^k + \eta(l\nabla f_i(w_0^k))$. Then by triangle inequality, we have
 1351

$$\begin{aligned}
 1352 \quad \|\Delta\| &= \left\| -\eta \sum_{l'=0}^{l-1} \nabla f_i(w_i^{t,l'}) + \eta l \nabla f_i(w_0^k) \right\| \\
 1353 \\
 1354 \\
 1355 \quad &= \eta \left\| \sum_{l'=0}^{l-1} \left(\nabla f_i(w_i^{k,l'}) - \nabla f_i(w_0^k) \right) \right\| \\
 1356 \\
 1357 \quad &\leq \eta \sum_{l'=0}^{l-1} \left\| f_i(w_i^{k,l'}) - \nabla f_i(w_0^k) \right\| \\
 1358 \\
 1359 \quad &\leq \eta \beta_i \sum_{l'=0}^{l-1} \|w_i^{k,l'} - w_0^k\| \\
 1360 \\
 1361 \quad &\leq \eta \beta_i \sum_{l'=0}^{l-1} \|w_i^{k,l'} - w_0^k\| \\
 1362 \\
 1363 \end{aligned} \tag{55}$$

1363 where β_i is the smoothness parameter of $f_i(w)$. Since each local dataset of a subset of global dataset,
 1364 $\forall i \in [1, M], \beta_i \leq \beta \sigma_{\max}$.
 1365

1366 In addition, since $\nabla f_i(w) = \sum_{s \in S_i} g'(x_s^T w) x_s$ we can have
 1367

$$\begin{aligned}
 1368 \quad &\|w_i^{k,l} - w_0^k\| \\
 1369 \quad &= \|w_i^{k,l} - w_0^k + \eta l \nabla f_i(w_0^k) - \eta l \nabla f_i(w_0^k)\| \\
 1370 \quad &\leq \|w_i^{k,l} - w_0^k + \eta l \nabla f_i(w_0^k)\| + \eta \|l \sum_{s \in S_i} g'(x_s^T w_0^k) x_s\| \\
 1371 \\
 1372 \quad &\leq \|\Delta\| + \eta l \sigma_{\max} \sqrt{\sum_{s \in S_i} (g'(x_s^T w_0^k))^2} \\
 1373 \\
 1374 \quad &\leq \|\Delta\| + \eta L \sigma_{\max} \sqrt{\sum_{s \in S} (g'(x_s^T w_0^k))^2} \\
 1375 \\
 1376 \quad &\leq \|\Delta\| + \frac{\eta L \sigma_{\max} M}{\gamma} \|f(w_0^k)\| \\
 1377 \\
 1378 \quad &\leq \|\Delta\| + \frac{\eta L \sigma_{\max} M}{\gamma} \|f(w_0^k)\| \\
 1379 \\
 1380 \end{aligned} \tag{56}$$

1380 where the second inequality is from the fact $\|\sum_{s \in S} a_s x_s\| \leq \sigma_{\max} \sqrt{\sum_{s \in S} a_s^2}$ for $\forall a_s \in \mathbb{R}$, the third
 1381 inequality is due to $S_i \subset S$, and the final inequality is from Lemma 5. Then we plug in $\|\Delta\|$ and get
 1382

$$\|\Delta\| \leq \eta \beta \sigma_{\max}^2 \sum_{l'=0}^{l-1} \|w_i^{k,l'} - w_0^k\| + \frac{\eta L \sigma_{\max} M}{\gamma} \|f(w_0^k)\|. \tag{57}$$

1386 Now we use another lemma from Nacson et al. (2019):
 1387

1388 **Lemma 7** (Lemma 4 in Nacson et al. (2019)). *Let ϵ and θ be positive constants. If $\delta_k \leq \theta + \epsilon \sum_{u=0}^{k-1} \delta_u$, then*
 1389

$$\delta_k \leq \frac{\theta}{1 - k\epsilon} \quad \text{and} \quad \sum_{u=0}^{k-1} \delta_u \leq \frac{k\theta}{1 - k\epsilon}.$$

1392 Directly applying this lemma to (57), we can obtain
 1393

$$\|w_i^{k,l} - w_0^k\| \leq \frac{\eta L \sigma_{\max} M}{\gamma (1 - l\eta \beta \sigma_{\max}^2)} \|\nabla f(w_0^k)\|. \tag{58}$$

1394 Then we further have
 1395

$$\|\Delta\| \leq \eta \beta \sigma_{\max}^2 \sum_{l'=0}^{l-1} \|w_i^{k,l'} - w_0^k\| \leq \frac{\eta^2 L \sigma_{\max}^3 \beta M l}{\gamma (1 - l\eta \beta \sigma_{\max}^2)} \|\nabla f(w_0^k)\|. \tag{59}$$

1400 By smoothness, we also have
 1401

$$\|\nabla f(w_i^{k,l}) - \nabla f(w_0^k)\| \leq \sigma_{\max}^2 \beta \|w_i^{k,l} - w_0^k\| \leq \frac{\eta L \sigma_{\max}^3 \beta M}{\gamma (1 - l\eta \beta \sigma_{\max}^2)} \|\nabla f(w_0^k)\|. \tag{60}$$

1403 \square

1404 C.2 PROOF OF CLAIM 2
1405

1406 In this section, we prove our implicit bias result. Recall that \hat{w} is the global max-margin solution defined
1407 in (4). We denote the set of support vectors in S as V . Thus the max-margin solution is $\hat{w} = \sum_{s \in S} \alpha_s x_s$,
1408 where $\alpha_s > 0, \forall s \in V; \alpha_s = 0, \forall s \notin V$. We further define a vector \tilde{w} , which satisfies

$$1409 \alpha_s = \eta \exp(-x_s^T \tilde{w}) \quad \forall s \in V. \quad (61)$$

1410 From Lemma 12 in Soudry et al. (2018), this solution exists for almost every dataset. We also denote
1411 the minimum margin to a non-support vector as

$$1412 \theta = \min_{s \notin V} x_s^T \hat{w} > 1. \quad (62)$$

1414 We will use the following Lemma:

1415 **Lemma 8.** *There exists $m_i(k, l)$ such that*

$$1417 L \sum_{u=1}^{k-1} \frac{1}{u} \frac{1}{M} \sum_{s \in V} \alpha_s x_s + \frac{l}{k} \sum_{s \in V_i} \alpha_s x_s = \frac{L}{M} \log(k) \hat{w} + \frac{L}{M} \zeta \hat{w} + m_i(k, l), \quad \forall l \in [1, L] \quad (63)$$

$$1420 \quad m_i(k+1, 0) \triangleq \frac{1}{M} \sum_{i=1}^M m_i(k, L), \quad \forall i \in [1, M] \quad (64)$$

1423 where $\|m_i(k, l)\| = o(k^{-1})$ and $\|m_i(k, l+1) - m_i(k, l)\| = O(k^{-1})$. ζ is Euler-Mascheroni constant,
1424 which is used to calculate $\sum_{u=1}^k \frac{1}{u} = \log k + \zeta + O(k^{-1})$.

1426 Now we define $r_i^{k, l}, \rho_i^{k, l}$ as

$$1427 \quad w_i^{k, l} = \log(Lk) \hat{w} + \rho_i^{k, l} \\ 1428 \quad = \log(Lk) \hat{w} + \tilde{w} + \frac{M}{L} m_i(k, l) + r_i^{k, l}, \quad \forall l \in [1, L]. \quad (65)$$

1431 Also, define $r_0^{k+1} = \frac{1}{M} \sum_{i=1}^M r_i^{k, L}$ and $\rho^{k+1} = \frac{1}{M} \sum_{i=1}^M \rho_i^{k, L}$. Thus

$$1433 \quad w_0^k = \frac{1}{M} \sum_{i=1}^M w_i^{k, L} = \log(Lk) \hat{w} + \rho^k = \log(Lk) \hat{w} + \tilde{w} + \frac{M}{L} \frac{1}{M} \sum_{i=1}^M m_i(k, l) + r_0^k \quad (66)$$

1435 We also define

$$1436 \quad \rho_i^{k, 0} = \rho^k, \quad r_i^{k, 0} = r_0^k \quad (67)$$

1437 Then for $l=0$, we have

$$1439 \quad w_i^{k+1, 0} = w_0^{k+1} = \log(Lk) \hat{w} + \tilde{w} + m_i(k+1, 0) + r_i^{k+1, 0}. \quad (68)$$

1440 We aim to bound $\|\rho^k\|$, and we can see that it is enough to prove $\|r_0^k\|$ is bounded to achieve this goal.

1442 We first write for a constant $k_1 > 0$ (defined later) and all $K \geq k_1$

$$1444 \quad \|r_0^K\|^2 - \|r_0^{k_1}\|^2 = \sum_{u=k_1}^K \|r_0^{u+1}\|^2 - \|r_0^u\|^2 \\ 1445 \quad \leq \sum_{u=k_1}^K \frac{1}{M} \sum_{i=1}^M \left(\|r_i^{u, L}\|^2 - \|r_i^{u, 0}\|^2 \right) \\ 1446 \quad = \frac{1}{M} \sum_{u=k_1}^K \sum_{l=0}^{L-1} \sum_{i=1}^M \|r_i^{u, l+1}\|^2 - \|r_i^{u, l}\|^2 \\ 1447 \quad = \frac{1}{M} \sum_{u=k_1}^K \sum_{l=0}^{L-1} \sum_{i=1}^M 2 \langle r_i^{u, l+1} - r_i^{u, l}, r_i^{u, l} \rangle + \|r_i^{u, l+1} - r_i^{u, l}\|^2 \quad (69)$$

1455 We will handle the inner product and squared norm items respectively. Here we need a lemma to
1456 characterize the behavior of inner product $\langle r_i^{u, l+1} - r_i^{u, l}, r_i^{u, l} \rangle$, which can be adapted from a lemma in
1457 Nacson et al. (2019) and its proof is omitted here:

1458
 1459 **Lemma 9** (Adapted from Lemma 6 in Nacson et al. (2019)). *Under Assumptions 1, 2, 3, $\exists \tilde{t}, C_1, C_2 > 0$
 1460 such that $\forall k > \tilde{k}$,*

1461
$$\langle r_i^{k,l+1} - r_i^{k,l}, r_i^{k,l} \rangle \leq C_1(Lk)^{-\theta} + \frac{C_2 M}{L} k^{-1-0.5\tilde{\mu}}, \forall l \in [0, L-1] \quad (70)$$

 1462

1463 , where $\tilde{\mu} = \min\{\mu_+, \mu_-, 0.25\}$.

1464
 1465 Let $a_i^{k,l} = \frac{M}{L} (m_i(k, l+1) - m_i(k, l))$ and we know $\|m_i(k, l+1) - m_i(k, l)\| = O(k^{-1})$ from Lemma 8.
 1466 Then we can handle the squared norm item:

1467
 1468
$$\begin{aligned} & \frac{1}{M} \sum_{u=k_1}^K \sum_{l=0}^{L-1} \sum_{i=1}^M \|r_i^{u,l+1} - r_i^{u,l}\|^2 \\ &= \frac{1}{M} \sum_{u=k_1}^K \sum_{l=0}^{L-1} \sum_{i=1}^M \|w_i^{k,l+1} - w_i^{k,l} - a_i^{k,l}\|^2 \\ &= \frac{1}{M} \sum_{u=k_1}^K \sum_{l=0}^{L-1} \sum_{i=1}^M \|w_i^{u,l+1} - w_i^{u,l}\|^2 + \frac{1}{M} \sum_{u=k_1}^K \sum_{l=0}^{L-1} \sum_{i=1}^M 2 \langle w_i^{u,l} - w_i^{u,l+1}, a_i^{u,l} \rangle + \frac{1}{M} \sum_{u=k_1}^K \sum_{l=0}^{L-1} \sum_{i=1}^M \|a_i^{u,l}\|^2 \\ &\leq \frac{1}{M} \sum_{u=k_1}^T \sum_{l=0}^{L-1} \sum_{i=1}^M \|w_i^{u,l+1} - w_i^{u,l}\|^2 + \frac{2}{M} \sqrt{\sum_{u=k_1}^K \sum_{l=0}^{L-1} \sum_{i=1}^M \|w_i^{u,l+1} - w_i^{u,l}\|^2 \sum_{u=k_1}^K \sum_{l=0}^{L-1} \sum_{i=1}^M \|a_i^{u,l}\|^2} \\ &\quad + \frac{1}{M} \sum_{u=k_1}^K \sum_{l=0}^{L-1} \sum_{i=1}^M \|a_i^{u,l}\|^2 \end{aligned} \quad (71)$$

 1483

1484 Since $\|a_i^{k,l}\| = O(\frac{M}{Lk})$, we can find a k_1 such that $\forall k \geq k_1, \forall l \in [0, L-1], \forall i \in [1, M]$ we have $\|a_i^{k,l}\| \leq \frac{M}{Lk}$.
 1485 Also, we know $\frac{1}{M} \sum_{k=k_1}^K \sum_{l=0}^{L-1} \sum_{i=1}^M \|w_i^{k,l+1} - w_i^{k,l}\|^2 < \infty$ from the proof of Claim 1 (53). Then we
 1486 can obtain

1487
 1488
$$\begin{aligned} & \frac{1}{M} \sum_{k=k_1}^K \sum_{l=0}^{L-1} \sum_{i=1}^M \|r_i^{k,l+1} - r_i^{k,l}\|^2 \\ &\leq \frac{1}{M} \sum_{k=k_1}^K \sum_{l=0}^{L-1} \sum_{i=1}^M \|w_i^{k,l+1} - w_i^{k,l}\|^2 + 2 \sqrt{\frac{1}{M} \sum_{k=k_1}^K \sum_{l=0}^{L-1} \sum_{i=1}^M \|w_i^{k,l+1} - w_i^{k,l}\|^2 \frac{1}{M} \sum_{k=k_1}^K \sum_{l=0}^{L-1} \sum_{i=1}^M \frac{M^2}{L^2} k^{-2}} \\ &\quad + \frac{1}{M} \sum_{k=k_1}^K \sum_{l=0}^{L-1} \sum_{i=1}^M \frac{M^2}{L^2} k^{-2} \\ &< \infty. \end{aligned} \quad (72)$$

 1498

1499 With Lemma 9 and the fact that $\forall c > 1, \sum_{u=1}^{\infty} u^{-c} < \infty$, we can finally get

1500
 1501
$$\|r_0^k\|^2 - \|r_0^{k_1}\|^2 \leq \frac{1}{M} \sum_{k=k_1}^K \sum_{l=0}^{L-1} \sum_{i=1}^M \left(2 \langle r_i^{u,l+1} - r_i^{u,l}, r_i^{u,l} \rangle + \|r_i^{u,l+1} - r_i^{u,l}\|^2 \right) < \infty. \quad (73)$$

 1502

1503 The $\|r_0^k\|^2$ is bounded, then $\|\rho^k\|$ is also bounded. We can know w_0^k converges to \hat{w} in direction:
 1504 $w_0^{k+1} = \log(Lk)\hat{w} + \rho^k$.

1505 Then we can analyze the dependence of $\|\rho^k\|$ on L . From (53) and the condition on learning rate
 1506 $\eta = O(L^{-1})$ we can know

1507
 1508
$$\frac{1}{M} \sum_{k=k_1}^K \sum_{l=0}^{L-1} \sum_{i=1}^M \|w_i^{k,l+1} - w_i^{k,l}\|^2 \leq O(L^{-1}) \sum_{k=0}^{\infty} \|\nabla f(w_0^k)\|^2. \quad (74)$$

 1509

1512 Then we can write 72 as
1513
1514
$$\frac{1}{M} \sum_{k=k_1}^K \sum_{l=0}^{L-1} \sum_{i=1}^M \|r_i^{k,l+1} - r_i^{k,l}\|^2$$

1515
1516
$$\leq O(L^{-1}) \sum_{k=k_1}^{\infty} \|\nabla f(w_0^k)\|^2 + 2 \sqrt{O(L^{-1}) \sum_{k=k_1}^{\infty} \|\nabla f(w_0^k)\|^2 \cdot \frac{M^2}{L} \sum_{k=k_1}^K k^{-2} + \frac{M^2}{L} \sum_{k=k_1}^K k^{-2}}$$

1517
1518
$$\leq O(L^{-1}) \left(\sum_{k=k_1}^{\infty} \|\nabla f(w_0^k)\|^2 + \sqrt{\sum_{k=k_1}^{\infty} \|\nabla f(w_0^k)\|^2 \sum_{k=k_1}^K k^{-2} + \sum_{k=k_1}^K k^{-2}} \right) \quad (75)$$

1519
1520
1521
1522
1523

1524
1525 From Lemma 9, since $\theta > 1$ we can know
1526
1527
$$\langle r_i^{k,l+1} - r_i^{k,l}, r_i^{k,l} \rangle \leq C_1(Lk)^{-\theta} + \frac{C_2 M}{L} k^{-1-0.5\bar{\mu}} = O(L^{-1})(k^{-\theta} + k^{-1-0.5\bar{\mu}}) \quad (76)$$

1528
1529

1530 Then we can obtain
1531
1532
$$\|r_0^k\|^2 - \|r_0^{k_1}\|^2$$

1533
1534
$$\leq \frac{1}{M} \sum_{k=k_1}^K \sum_{l=0}^{L-1} \sum_{i=1}^M \left(2 \langle r_i^{u,l+1} - r_i^{u,l}, r_i^{u,l} \rangle + \|r_i^{u,l+1} - r_i^{u,l}\|^2 \right)$$

1535
1536
$$\leq O(1) \sum_{k=k_1}^K (k^{-\theta} + k^{-1-0.5\bar{\mu}}) + O(L^{-1}) \left(\sum_{k=k_1}^{\infty} \|\nabla f(w_0^k)\|^2 + \sqrt{\sum_{k=k_1}^{\infty} \|\nabla f(w_0^k)\|^2 \sum_{k=k_1}^K k^{-2} + \sum_{k=k_1}^K k^{-2}} \right)$$

1537
1538
1539
$$< \infty \quad (77)$$

1540

1541 and the dominating term on L is $O(1)$. By definition $\rho_i^{k,l} = \log(Lk)\hat{w} + \hat{w} + \frac{M}{L}m_i(k,l) + r_i^{k,l}$, we can get
1542 $\|\rho_i^{k,l}\|$ is bounded with $k \rightarrow \infty$ and $O(1)$ on L .
1543

1544 Now we can get the convergence rate of the direction.

1545
1546
$$\frac{w_0^{k+1}}{\|w_0^{k+1}\|}$$

1547
1548
$$= \frac{\log(Lk)\hat{w} + \rho^k}{\sqrt{\rho^{kT}\rho^k + \hat{w}^T\hat{w}\log^2(Lk) + 2\rho^{kT}\hat{w}\log(Lk)}}$$

1549
1550
1551
$$= \frac{\rho^k / \log(Lk) + \hat{w}}{\|\hat{w}\| \sqrt{1 + \frac{2\rho^{kT}\hat{w}}{\|\hat{w}\|^2\log(Lk)} + \frac{\|\rho^k\|^2}{\|\hat{w}\|^2\log^2(Lk)}}}$$

1552
1553
1554
$$= \frac{1}{\|\hat{w}\|} \left(\frac{\rho^k}{\log(Lk)} + \hat{w} \right) \left[1 - \frac{\rho^{kT}\hat{w}}{\|\hat{w}\|^2\log(Lk)} + \left(\frac{3}{2} \left(\frac{\rho^{kT}\hat{w}}{\|\hat{w}\|^2} \right)^2 - \frac{\|\rho^k\|^2}{2\|\hat{w}\|^2} \right) \frac{1}{\log^2(Lk)} + O\left(\frac{1}{\log^3(Lk)}\right) \right]$$

1555
1556
1557
$$= \frac{\hat{w}}{\|\hat{w}\|} + \left(\frac{\rho^k}{\|\hat{w}\|} - \frac{\hat{w}}{\|\hat{w}\|} \frac{\rho^{kT}\hat{w}}{\|\hat{w}\|^2} \right) \frac{1}{\log(Lk)} + O\left(\frac{1}{\log^2(Lk)}\right)$$

1558
1559
1560
$$= \frac{\hat{w}}{\|\hat{w}\|} + \left(I - \frac{\hat{w}\hat{w}^T}{\|\hat{w}\|^2} \right) \frac{\rho^k}{\|\hat{w}\|} \frac{1}{\log(Lk)} + O\left(\frac{1}{\log^2(Lk)}\right), \quad (78)$$

1561

1562 where the third equality is from $\frac{1}{\sqrt{1+x}} = 1 - \frac{1}{2}x + \frac{3}{4}x^2 + O(x^3)$. Thus we can get
1563

1564
1565
$$\left\| \frac{w_0^k}{\|w_0^k\|} - \frac{\hat{w}}{\|\hat{w}\|} \right\| = O\left(\frac{1}{\log(Lk)}\right). \quad (79)$$

1566 C.2.1 PROOF OF LEMMA 8
15671568 *Proof.* We first write

$$\begin{aligned}
& L \sum_{u=1}^{k-1} \frac{1}{u} \frac{1}{M} \sum_{s \in V} \alpha_s x_s + \frac{l}{k} \sum_{s \in V_i} \alpha_s x_s \\
&= \frac{L}{M} \hat{w} \sum_{u=1}^{k-1} \frac{1}{u} + \frac{l}{k} \sum_{s \in V_i} \alpha_s x_s \\
&= \frac{L}{M} \hat{w} (\log(k) + \zeta + O(k^{-1})) + \frac{l}{k} \sum_{s \in V_i} \alpha_s x_s \\
&= \frac{L}{M} \log(k) \hat{w} + \frac{L\zeta}{M} \hat{w} + O(k^{-1}) \hat{w} + \frac{l}{k} \sum_{s \in V_i} \alpha_s x_s,
\end{aligned} \tag{80}$$

1581 where the first equality is definition of \hat{w} , the second equality is from the fact

1582
$$\sum_{u=1}^k \frac{1}{u} = \log k + \zeta + O(k^{-1}) \tag{81}$$

1583 and $\log k - \log(k-1) = O(k^{-1})$. $\tag{82}$

1584 Then we define

1585
$$m_i(k, l) = L \sum_{u=1}^{k-1} \frac{1}{u} \frac{1}{M} \sum_{s \in V} \alpha_s x_s + \frac{l}{k} \sum_{s \in V_i} \alpha_s x_s - \frac{L}{M} \log(k) \hat{w} - \frac{L\zeta}{M} \hat{w}, \quad \forall l \in [1, L] \tag{83}$$

1586 and

1587
$$m_i(k+1, 0) = \frac{1}{M} \sum_{i=1}^M m_i(k, L) = L \sum_{u=1}^k \frac{1}{u} \frac{1}{M} \sum_{s \in V} \alpha_s x_s - \frac{L}{M} \log(k) \hat{w} - \frac{L\zeta}{M} \hat{w}, \quad \forall i \in [1, M]. \tag{84}$$

1588 We can obviously see $\|m_i(k, l)\| = O(k^{-1})$. For the difference, we can get

1589
$$\|m_i(k, l+1) - m_i(k, l)\| = \left\| \frac{1}{k} \sum_{s \in V_i} \alpha_s x_s \right\| = O(k^{-1}), \quad \forall l \in [1, L-1] \tag{85}$$

1590
$$\|m_i(k, 1) - m_i(k, 0)\| = \left\| \frac{1}{k} \sum_{s \in V_i} \alpha_s x_s - \frac{L}{M} (\log(k+1) - \log k) \right\| = O(k^{-1}). \tag{86}$$

1602 \square

1603 C.3 PROOF OF CLAIM 3

1604 In the proof of Claim 1, we already know $f(w_0^k)$ would continue to decrease to zero when $k \rightarrow \infty$. Now
1605 we establish the convergence rate of $f(w_0^k)$. Recall V is the set of support vectors and θ is the minimum
1606 margin for non-support vectors. From Assumptions 2 and 3, we can get

$$\begin{aligned}
f(w_0^k) &\leq \frac{1}{M} \sum_{s \in S} (1 + \exp(-\mu_+ x_s^T w_0^k)) \exp(-x_s^T w_0^k) \\
&= \frac{1}{M} \sum_{s \in S} (1 + \exp(-\mu_+ x_s^T (\hat{w} \log(Lk) + \rho^k))) \exp(-x_s^T (\hat{w} \log(Lk) + \rho^k)) \\
&= \frac{1}{M} \sum_{s \in S} \left(1 + (Lk)^{-\mu_+ x_s^T \hat{w}} \exp(-\mu_+ x_s^T \rho^k) \right) \exp(-x_s^T \rho^k) (Lk)^{-x_s^T \hat{w}} \\
&= \frac{1}{M} \sum_{s \in S} \left[\exp(-x_s^T \rho^k) (Lk)^{-x_s^T \hat{w}} + (Lk)^{-\mu_+ x_s^T \hat{w}} \exp(-\mu_+ x_s^T \rho^k) \exp(-x_s^T \rho^k) (Lk)^{-x_s^T \hat{w}} \right]
\end{aligned} \tag{87}$$

1620 We can divide the dataset S into set V with support vectors and the complementary set. For samples in
 1621 the set V , we have $x_s^T \hat{w} = 1$ and we can write
 1622

$$\begin{aligned} 1623 & \sum_{s \in V} \exp(-x_s^T \rho^k) (Lk)^{-x_s^T \hat{w}} + (Lk)^{-\mu_+ x_s^T \hat{w}} \exp(-\mu_+ x_s^T \rho^k) \exp(-x_s^T \rho^k) (Lk)^{-x_s^T \hat{w}} \\ 1624 & = \sum_{s \in V} \frac{1}{Lk} \exp(-x_s^T \rho^k) + \frac{1}{(Lk)^{1+\mu_+}} \exp(-(1+\mu_+) x_s^T \rho^k) \end{aligned} \quad (88)$$

1625 For samples not in the set V , we have $x_s^T \hat{w} \geq \theta$ since θ is the minimum margin for non-support vectors.
 1626 Then we can write
 1627

$$\begin{aligned} 1628 & \sum_{s \notin V} \exp(-x_s^T \rho^k) (Lk)^{-x_s^T \hat{w}} + (Lk)^{-\mu_+ x_s^T \hat{w}} \exp(-\mu_+ x_s^T \rho^k) \exp(-x_s^T \rho^k) (Lk)^{-x_s^T \hat{w}} \\ 1629 & \leq \sum_{s \notin V} \frac{1}{(Lk)^\theta} \exp(-x_s^T \rho^k) + \frac{1}{(Lk)^{(1+\mu_+)\theta}} \exp(-(1+\mu_+) x_s^T \rho^k) \end{aligned} \quad (89)$$

1630 Combining the two terms, we can have
 1631

$$\begin{aligned} 1632 & f(w_0^k) \leq \frac{1}{M} \sum_{s \in S} \left[\exp(-x_s^T \rho^k) (Lk)^{-x_s^T \hat{w}} + (Lk)^{-\mu_+ x_s^T \hat{w}} \exp(-\mu_+ x_s^T \rho^k) \exp(-x_s^T \rho^k) (Lk)^{-x_s^T \hat{w}} \right] \\ 1633 & = \left[\frac{1}{MLk} \sum_{s \in V} \exp(-x_s^T \rho^k) \right] + O((Lk)^{-\max(\theta, 1+\mu_+)}). \end{aligned} \quad (90)$$

1634 Thus the training loss $f(w_0^k) = O(\frac{1}{Lk})$.
 1635
 1636
 1637
 1638
 1639
 1640
 1641
 1642
 1643
 1644
 1645
 1646
 1647
 1648
 1649
 1650
 1651
 1652
 1653
 1654
 1655
 1656
 1657
 1658
 1659
 1660
 1661
 1662
 1663
 1664
 1665
 1666
 1667
 1668
 1669
 1670
 1671
 1672
 1673

1674 **D PROOFS**1675 **OF IMPLICIT BIAS WITH LEARNING RATE INDEPENDENT OF L IN SECTION 4**

1676 In this section we also redefine the samples $y_{ij}x_{ij}$ to x_{ij} to subsume the labels. With abuse of notation,
 1677 we use S_i to denote the set of support vectors in i -th compute node and S is the set of support vectors
 1678 in global dataset. The number of samples N is identical for all the compute nodes, and the local dataset
 1679 is $\{x_{ij}, y_{ij}\}_{j=1}^N$. Since the loss function is fixed as exponential loss in this section, the β in this section
 1680 refers coefficient of support vectors, not smoothness parameter.

1681 **D.1 PROOFS OF LEMMA 1**

1682 We assume $\|w_0^k - \ln(\frac{1}{\lambda})\bar{w}_0^k\| = O(k \ln \ln \frac{1}{\lambda})$. In this case, since $\ln \frac{1}{\lambda}$ grows faster, when $\lambda \rightarrow 0$, we can have
 1683 $\lim_{\lambda \rightarrow 0} \frac{w_0^k}{\|w_0^k\|} = \frac{\bar{w}_0^k}{\|\bar{w}_0^k\|}$ for any k at order $O\left(\frac{\ln(1/\lambda)}{\ln \ln(1/\lambda)}\right)$. We will prove it by induction. We define global
 1684 and local residuals as $r^k = w_0^k - \ln(\frac{1}{\lambda})\bar{w}_0^k$ and $r_i^k = w_i^k - \ln(\frac{1}{\lambda})\bar{w}_i^k$.

1685 When $k=0$, since $w_0^0 = \bar{w}_0^0 = 0$, $r_i^0 = 0$ and the assumption trivially holds.

1686 When $k \geq 1$, we have

$$\begin{aligned} \|r^k\| &= \left\| w_0^k - \ln\left(\frac{1}{\lambda}\right)\bar{w}_0^k \right\| = \frac{1}{M} \left\| \sum_{i=1}^M w_i^k - \ln\left(\frac{1}{\lambda}\right)\bar{w}_i^k \right\| \\ &\leq \frac{1}{M} \sum_{i=1}^M \left\| w_i^k - \ln\left(\frac{1}{\lambda}\right)\bar{w}_i^k \right\| = \frac{1}{M} \sum_{i=1}^M \|r_i^k\|. \end{aligned} \quad (91)$$

1687 where the inequality is triangle inequality. We then focus on the local residual r_i^k . We choose an $O(1)$
 1688 vector \tilde{w}_i^k and a sign $s_i^k \in \{-1, +1\}$ to show

$$\begin{aligned} \|r_i^k\| &= \left\| w_i^k - \left[\left(\ln\left(\frac{1}{\lambda}\right) + s_i^k \ln \ln\left(\frac{1}{\lambda}\right) \right) \bar{w}_i^k + \tilde{w}_i^k \right] + s_i^k \ln \ln\left(\frac{1}{\lambda}\right) \bar{w}_i^k + \tilde{w}_i^k \right\| \\ &\leq \left\| w_i^k - \left[\left(\ln\left(\frac{1}{\lambda}\right) + s_i^k \ln \ln\left(\frac{1}{\lambda}\right) \right) \bar{w}_i^k + \tilde{w}_i^k \right] \right\| + \ln \ln\left(\frac{1}{\lambda}\right) \|\bar{w}_i^k\| + \|\tilde{w}_i^k\| \end{aligned} \quad (92)$$

1689 Recall the w_i^k is the solution of optimization problem

$$\operatorname{argmin}_{w_i} f_i(w_i) = \sum_{j=1}^N \exp(-x_{ij}^T w_i) + \frac{\lambda}{2} \|w_i - w_0^{k-1}\|^2, \quad (93)$$

1690 and the loss function $f_i(w_i)$ is a λ -strongly convex function. Thus we have

$$\|w_i^k - w\| \leq \frac{1}{\lambda} \|\nabla f_i(w)\|, \quad \text{for any } w. \quad (94)$$

1691 Then back to 92, we have

$$\|r_i^k\| \leq \frac{1}{\lambda} \underbrace{\left\| \nabla f_i \left[\left(\ln\left(\frac{1}{\lambda}\right) + s_i^k \ln \ln\left(\frac{1}{\lambda}\right) \right) \bar{w}_i^k + \tilde{w}_i^k \right] \right\|}_{\|A_i\|} + \ln \ln\left(\frac{1}{\lambda}\right) \|\bar{w}_i^k\| + \|\tilde{w}_i^k\|. \quad (95)$$

1692 Next we need to show the first term A_i is at $O((k-1) \ln \ln(\frac{1}{\lambda}))$, and also since $\|\bar{w}_i^k\|$ and $\|\tilde{w}_i^k\|$ are $O(1)$
 1693 vectors, then $\|r_i^k\|$ is at order $O(k \ln \ln(\frac{1}{\lambda}))$. After averaging, $\|r^k\|$ is also at order $O(k \ln \ln(\frac{1}{\lambda}))$. This
 1694 confirms the assumption made for induction.

1695 Now we focus on the term A_i . The gradient of function $f_i(w)$ is

$$\nabla f_i(w_i) = \sum_j -x_{ij} \exp(-x_{ij}^T w_i) + \lambda (w_i - w_0^{k-1}). \quad (96)$$

1728 The term A_i is
 1729

$$\begin{aligned}
 1730 \quad A_i &= \frac{1}{\lambda} \nabla f_i \left[\left(\ln\left(\frac{1}{\lambda}\right) + s_i^k \ln \ln\left(\frac{1}{\lambda}\right) \right) \bar{w}_i^k + \tilde{w}_i^k \right] \\
 1731 \\
 1732 &= -\frac{1}{\lambda} \sum_j x_{ij} \exp\left(x_{ij}^T \ln\left(\lambda \ln^{-s_i^k}\left(\frac{1}{\lambda}\right)\right) \bar{w}_i^k\right) \exp(-x_{ij}^T \tilde{w}_i^k) + \left(\ln\left(\frac{1}{\lambda}\right) + s_i^k \ln \ln\left(\frac{1}{\lambda}\right) \right) \bar{w}_i^k + \tilde{w}_i^k - w_0^{k-1} \\
 1733 \\
 1734 &= -\frac{1}{\lambda} \sum_j x_{ij} \left(\lambda \ln^{-s_i^k}\left(\frac{1}{\lambda}\right) \right)^{x_{ij}^T \bar{w}_i^k} \exp(-x_{ij}^T \tilde{w}_i^k) + \left(\ln\left(\frac{1}{\lambda}\right) + s_i^k \ln \ln\left(\frac{1}{\lambda}\right) \right) \bar{w}_i^k + \tilde{w}_i^k - w_0^{k-1}. \quad (97)
 1735 \\
 1736 \\
 1737
 \end{aligned}$$

1738 Then we define the set of support vectors as $S_i^k = \{x_{ij} | x_{ij}^T \bar{w}_i^k = 1\}$. Recall that we assume
 1739 $r^{k-1} = w_0^{k-1} - \ln\left(\frac{1}{\lambda}\right) \bar{w}_0^{k-1}$ is at order $O((k-1) \ln \ln\left(\frac{1}{\lambda}\right))$. We can obtain
 1740

$$\begin{aligned}
 1741 \quad A_i &= -\frac{1}{\lambda} \left(\lambda \ln^{-s_i^k}\left(\frac{1}{\lambda}\right) \right)^1 \sum_{x_{ij} \in S_i^k} x_{ij} \exp(-x_{ij}^T \tilde{w}_i^k) - \frac{1}{\lambda} \sum_{x_{ij} \notin S_i^k} x_{ij} \left(\lambda \ln^{-s_i^k}\left(\frac{1}{\lambda}\right) \right)^{x_{ij}^T \bar{w}_i^k} \exp(-x_{ij}^T \tilde{w}_i^k) \\
 1742 \\
 1743 &\quad + \ln\left(\frac{1}{\lambda}\right) (\bar{w}_i^k - \bar{w}_0^{k-1}) - r^{k-1} + s_i^k \ln \ln\left(\frac{1}{\lambda}\right) \bar{w}_i^k + \tilde{w}_i^k \\
 1744 \\
 1745 &= -\ln^{-s_i^k}\left(\frac{1}{\lambda}\right) \sum_{x_{ij} \in S_i^k} x_{ij} \exp(-x_{ij}^T \tilde{w}_i^k) - \sum_{x_{ij} \notin S_i^k} x_{ij} \lambda^{x_{ij}^T \bar{w}_i^k - 1} \left(\ln\left(\frac{1}{\lambda}\right) \right)^{-s_i^k x_{ij}^T \bar{w}_i^k} \exp(-x_{ij}^T \tilde{w}_i^k) \\
 1746 \\
 1747 &\quad + \ln\left(\frac{1}{\lambda}\right) (\bar{w}_i^k - \bar{w}_0^{k-1}) - r^{k-1} + s_i^k \ln \ln\left(\frac{1}{\lambda}\right) \bar{w}_i^k + \tilde{w}_i^k. \quad (98)
 1748 \\
 1749 \\
 1750 \\
 1751
 \end{aligned}$$

1752 By the triangle inequality, we have

$$\begin{aligned}
 1753 \quad \|A_i\| &\leq \underbrace{\left\| \ln\left(\frac{1}{\lambda}\right) (\bar{w}_i^k - \bar{w}_0^{k-1}) - \ln^{-s_i^k}\left(\frac{1}{\lambda}\right) \sum_{x_{ij} \in S_i^k} x_{ij} \exp(-x_{ij}^T \tilde{w}_i^k) \right\|}_{B_1} \\
 1754 \\
 1755 &\quad + \underbrace{\left\| \sum_{x_{ij} \notin S_i^k} x_{ij} \lambda^{x_{ij}^T \bar{w}_i^k - 1} \left(\ln\left(\frac{1}{\lambda}\right) \right)^{-s_i^k x_{ij}^T \bar{w}_i^k} \exp(-x_{ij}^T \tilde{w}_i^k) \right\|}_{B_2} \\
 1756 \\
 1757 &\quad + \underbrace{\left\| r^{k-1} \right\|}_{O((k-1) \ln \ln\left(\frac{1}{\lambda}\right))} + \underbrace{\ln \ln\left(\frac{1}{\lambda}\right) \left\| \bar{w}_i^k \right\|}_{O(1)} + \underbrace{\left\| \tilde{w}_i^k \right\|}_{O(1)}. \quad (99)
 1758 \\
 1759 \\
 1760 \\
 1761 \\
 1762 \\
 1763 \\
 1764 \\
 1765
 \end{aligned}$$

1766 We just need to show B_1 and B_2 approach to 0 then $\|A_i\|$ can approach to $O(k \ln \ln\left(\frac{1}{\lambda}\right))$.

1767 We divide it into two cases.

1768 1. When $\bar{w}_i^k = P(\bar{w}_0^{k-1}) \neq \bar{w}_0^{k-1}$, meaning \bar{w}_0^{k-1} is not in the convex set C_i . In this case we choose
 1769 $s_i^k = -1$ then
 1770

$$\begin{aligned}
 1771 \quad B_1 &= \left\| \ln\left(\frac{1}{\lambda}\right) (\bar{w}_i^k - \bar{w}_0^{k-1}) - \ln\left(\frac{1}{\lambda}\right) \sum_{x_{ij} \in S_i^k} x_{ij} \exp(-x_{ij}^T \tilde{w}_i^k) \right\| \\
 1772 \\
 1773 &= \ln\left(\frac{1}{\lambda}\right) \left\| (\bar{w}_i^k - \bar{w}_0^{k-1}) - \sum_{x_{ij} \in S_i^k} x_{ij} \exp(-x_{ij}^T \tilde{w}_i^k) \right\|. \quad (100)
 1774 \\
 1775 \\
 1776 \\
 1777
 \end{aligned}$$

1778 We now want to choose \tilde{w}_i^k to make B_1 as 0. Since \bar{w}_i^k is the solution of SVM problem (9), by the KKT
 1779 condition of SVM problem, it can be written as

$$\bar{w}_i^k = \bar{w}_0^{k-1} + \sum_{x_{ij} \in S_i^k} \beta_{ij} x_{ij} \quad (101)$$

1782 where β_{ij} is the dual variable corresponding to x_{ij} in the set of support vectors. Thus we want to choose \tilde{w}_i^k as
 1783

$$1784 \sum_{x_{ij} \in S_i^k} \exp(-x_{ij}^T \tilde{w}_i^k) x_{ij} = \sum_{x_{ij} \in S_i^k} \beta_{ij} x_{ij}. \quad (102)$$

1787 We can prove such a \tilde{w}_i^k almost surely exists in Lemma 10.

1788 For the term B_2 , since $\lim_{\lambda \rightarrow 0} \lambda^{c-1} \ln^c(\frac{1}{\lambda}) \rightarrow 0$ for any constant $c > 1$, and $x_{ij}^T \bar{w}_i^k - 1 > 0$ for any x_{ij}
 1789 being not a support vector, then we can see
 1790

$$1791 B_2 = \left\| \sum_{x_{ij} \notin S_i^k} x_{ij} \lambda^{x_{ij}^T \bar{w}_i^k - 1} \left(\ln\left(\frac{1}{\lambda}\right) \right)^{x_{ij}^T \bar{w}_i^k} \exp(-x_{ij}^T \bar{w}_i^k) \right\| \xrightarrow{\lambda \rightarrow 0} 0. \quad (103)$$

1794 Here we choose \tilde{w}_i^k and s_i^k to make $B_1 = 0$ and $B_2 \rightarrow 0$.

1795 2. When $\bar{w}_i^k = P(\bar{w}_0^{k-1}) = \bar{w}_0^{k-1}$, meaning \bar{w}_0^{k-1} is already in the convex set C_i . Then $\bar{w}_i^k - \bar{w}_0^{k-1} = 0$.
 1796 In this case we choose $\tilde{w}_i^k = 0$ and $s_i^k = +1$. We can have
 1797

$$1799 B_1 = \ln^{-1}\left(\frac{1}{\lambda}\right) \left\| \sum_{x_{ij} \in S_i^k} x_{ij} \right\| \xrightarrow{\lambda \rightarrow 0}, \quad (104)$$

1802 since $\ln^{-1}\left(\frac{1}{\lambda}\right) \xrightarrow{\lambda \rightarrow 0} 0$ and $\left\| \sum_{x_{ij} \in S_i^k} x_{ij} \right\|$ is $O(1)$.

1805 And since $x_{ij}^T \bar{w}_i^k - 1 > 0$ for any x_{ij} being not a support vector, we have

$$1807 B_2 = \left\| \sum_{x_{ij} \notin S_i^k} x_{ij} \lambda^{x_{ij}^T \bar{w}_i^k - 1} \left(\ln\left(\frac{1}{\lambda}\right) \right)^{-x_{ij}^T \bar{w}_i^k} \right\| \xrightarrow{\lambda \rightarrow 0} 0, \quad (105)$$

1810 where $\lambda^{x_{ij}^T \bar{w}_i^k - 1} \xrightarrow{\lambda \rightarrow 0} 0$ and $\left(\ln\left(\frac{1}{\lambda}\right) \right)^{-x_{ij}^T \bar{w}_i^k} \xrightarrow{\lambda \rightarrow 0} 0$. Thus we choose \tilde{w}_i^k and s_i^k to make $B_1 \rightarrow 0$ and
 1811 $B_2 \rightarrow 0$.
 1812

1813 Plugging 99 back into 95, we can obtain

$$1815 \|r_i^k\| \leq \|A_i^k\| + \ln \ln\left(\frac{1}{\lambda}\right) \|\bar{w}_i^k\| + \|\tilde{w}_i^k\| \\ 1816 \leq \underbrace{B_1 + B_2}_{\rightarrow 0} + 2 \ln \ln\left(\frac{1}{\lambda}\right) \|\bar{w}_i^k\| + 2 \|\tilde{w}_i^k\| + \|r^{k-1}\| \\ 1817 \leq 2 \ln \ln\left(\frac{1}{\lambda}\right) \|\bar{w}_i^k\| + 2 \|\tilde{w}_i^k\| + \|r^{k-1}\|. \quad (106)$$

1821 By the assumption $\|r^{k-1}\| = O((k-1) \ln \ln(\frac{1}{\lambda}))$ and $\|\bar{w}_i^k\| = O(1)$, $\|\tilde{w}_i^k\| = O(1)$, we have
 1822 $\|r_i^k\| = O(k \ln \ln(\frac{1}{\lambda}))$.
 1823

1824 From 91, we finally obtain
 1825

$$1826 \|r^k\| \leq \frac{1}{M} \|r_i^k\| = O(k \ln \ln(\frac{1}{\lambda})), \quad (107)$$

1828 which confirms our assumption. Then we have $\lim_{\lambda \rightarrow 0} \frac{w_0^k}{\|w_0^k\|} = \frac{\bar{w}_0^k}{\|\bar{w}_0^k\|}$ for any k at order $o\left(\frac{\ln(1/\lambda)}{\ln \ln(1/\lambda)}\right)$.
 1829

1831 D.2 PROOFS OF AUXILIARY LEMMAS

1832 **Lemma 10.** For the sequence $\{\bar{w}_0^k\}$ generated by sequential SVM problems 9 and aggregations, and
 1833 for almost all datasets sampled from M continuous distributions, the unique dual solution $\beta_i^k \in \mathbb{R}^{|S_i| \times 1}$
 1834 satisfying the KKT conditions of SVM problem 9 has non-zero elements. Then there exists \tilde{w}_i^k satisfying
 1835 $X_{S_i} \tilde{w}_i^k = -\ln \beta_i^k$.

For almost all datasets, a hyperplane can be determined by d points. Thus there are at most d support vectors and the set of support vectors is linearly independent.

Proof. By the KKT condition of SVM problem, we can write the solution as

$$\bar{w}_i^k = \bar{w}_0^{k-1} + \sum_{x_{ij} \in S_i} \beta_{ij}^k x_{ij} = \bar{w}_0^{k-1} + X_{S_i}^T \beta_i^k. \quad (108)$$

where $X_{S_i} \in \mathbb{R}^{|S_i| \times d}$ is the data matrix with all the support vectors, and $\beta_i^k \in \mathbb{R}^{|S_i| \times 1}$ is the dual variable vector. Thus we can obtain

$$\beta_i^k = (X_{S_i} X_{S_i}^T)^{-1} X_{S_i} (\bar{w}_i^k - \bar{w}_0^{k-1}) = (X_{S_i} X_{S_i}^T)^{-1} \mathbf{1}_{S_i} - (X_{S_i} X_{S_i}^T)^{-1} X_{S_i} \bar{w}_0^{k-1}, \quad (109)$$

where $X_{S_i} X_{S_i}^T$ is invertible since X_{S_i} has full row rank $|S_i|$, and the second equality is from $X_{S_i} \bar{w}_i^k = \mathbf{1}_{S_i}$ with $\mathbf{1}_{S_i} \in \mathbb{R}^{|S_i| \times 1}$ being all one vector. Plugging β_i^k back, we have

$$\bar{w}_i^k = \left[I - X_{S_i}^T (X_{S_i} X_{S_i}^T)^{-1} X_{S_i} \right] \bar{w}_0^{k-1} + X_{S_i}^T (X_{S_i} X_{S_i}^T)^{-1} \mathbf{1}_{S_i}. \quad (110)$$

After averaging, the global model is

$$\bar{w}_0^k = \left[I - \frac{1}{M} \sum_{i=1}^M X_{S_i}^T (X_{S_i} X_{S_i}^T)^{-1} X_{S_i} \right] \bar{w}_0^{k-1} + \frac{1}{M} \sum_{i=1}^M X_{S_i}^T (X_{S_i} X_{S_i}^T)^{-1} \mathbf{1}_{S_i}. \quad (111)$$

It implies \bar{w}_0^k is a rational function in the components of X_1, X_2, \dots, X_M , and also β_i^k is also a rational function in the components of data matrices. So its entries can be expressed as $\beta_{ij}^k = p_{ij}^k(X_1, X_2, \dots, X_M) / q_{ij}^k(X_1, X_2, \dots, X_M)$ for some polynomials p_{ij}^k, q_{ij}^k . Note that $\beta_{ij}^k = 0$ only if $p_{ij}^k(X_1, X_2, \dots, X_M) = 0$, and the components of X_1, X_2, \dots, X_M must constitute a root of polynomial p_{ij}^k . However, the root of any polynomial has measure zero, unless the polynomial is the zero polynomial, i.e., $p_{ij}^k(X_1, X_2, \dots, X_M) = 0$ for any X_1, X_2, \dots, X_M .

Next we need to show p_{ij}^k cannot be zero polynomials. To do this, we just need to construct a specific X_1, X_2, \dots, X_M where the p_{ij}^k is not zero polynomial. Denote $e_i \in \mathbb{R}^d$ as the i -th standard unit vector, and v_1, v_2, \dots, v_M be the number of support vectors at M compute nodes. We construct the datasets as

$$X_i = r_i [e_1, e_2, \dots, e_{v_i}]^T, \text{ for all } i. \quad (112)$$

where r_i are positive constants that will be chosen later. For these datasets, the set of support vector is dataset itself, i.e., $X_{S_i} = X_i$. We can calculate

$$X_i X_i^T = r_i^2 I_{v_i}, X_i^T X_i = r_i^2 \begin{bmatrix} I_{v_i} & \mathbf{0} \\ \mathbf{0} & \mathbf{0}_{(d-v_i) \times (d-v_i)} \end{bmatrix}, X_i^T \mathbf{1}_{S_i} = r_i \begin{bmatrix} \mathbf{1}_{v_i} \\ \mathbf{0}_{d-v_i} \end{bmatrix} \quad (113)$$

Thus we have

$$\bar{w}_i^k = \left(I_d - \begin{bmatrix} I_{v_i} & \mathbf{0} \\ \mathbf{0} & \mathbf{0}_{(d-v_i) \times (d-v_i)} \end{bmatrix} \right) \bar{w}_0^{k-1} + \frac{1}{r_i} \begin{bmatrix} \mathbf{1}_{v_i} \\ \mathbf{0}_{d-v_i} \end{bmatrix}. \quad (114)$$

After averaging, the global model in 111 becomes

$$\bar{w}_0^k = \underbrace{\begin{bmatrix} 0 & & & & \\ & \ddots & & & \\ & & 0 & & \\ & & & a_1 & \\ & & & & \ddots \\ & & & & & a_{v_{\max}-v_{\min}} & \\ & & & & & & 1 & \\ & & & & & & & \ddots \\ & & & & & & & & 1 \end{bmatrix}}_A \bar{w}_0^{k-1} + \underbrace{\begin{bmatrix} b_1 \\ \vdots \\ b_{v_{\max}} \\ \mathbf{0}_{d-v_{\max}} \end{bmatrix}}_b. \quad (115)$$

1890 where $a_j \in \{\frac{1}{M}, \frac{2}{M}, \dots, \frac{M-1}{M}\}$ is a constant in the range (0,1), $b_j = \frac{1}{M} \sum_{i \in B_j} \frac{1}{r_i}$ is a positive constant and
 1891 $B_j \in [M]$ is a set consisting of some compute nodes. Note that A and b are fixed in the iterations and
 1892 A is a diagonal matrix.

1893 By recursively applying $\bar{w}_0^k = A\bar{w}_0^{k-1} + b$, due to $\bar{w}_0^0 = 0$, we can obtain

$$1894 \quad \bar{w}_0^k = (I + A + A^2 + \dots + A^{k-1})b. \quad (116)$$

1895 Since A is diagonal, the summation is

$$1896 \quad \sum_{j=0}^{k-1} A^j = \begin{bmatrix} 1 & & & & & & & \\ & \ddots & & & & & & \\ & & 1 & & & & & \\ & & & \sum_{j=0}^{k-1} a_1^j & & & & \\ & & & & \ddots & & & \\ & & & & & \sum_{j=0}^{k-1} a_{v_{\max}-v_{\min}}^j & & \\ & & & & & & k & \\ & & & & & & & \ddots \\ & & & & & & & & k \end{bmatrix} \quad (117)$$

1897 Recall that

$$1898 \quad \beta_i^k = (X_i X_i^T)^{-1} \mathbf{1}_{v_i} - (X_i X_i^T)^{-1} X_i \bar{w}_0^{k-1} \\ 1899 \quad = \frac{1}{r_i^2} \mathbf{1}_{v_i} - \frac{1}{r_i^2} (\bar{w}_0^{k-1})_{v_i} = \frac{1}{r_i^2} (\mathbf{1}_{v_i} - (\bar{w}_0^{k-1})_{v_i}). \quad (118)$$

1900 where $(\bar{w}_0^{k-1})_{v_i}$ is the vector with first v_i elements of \bar{w}_0^{k-1} .

1901 We need every element of β_i^k to be positive, so that we require every element of $(\bar{w}_0^{k-1})_{v_i}$ is less than
 1902 1. Then it holds for any i -th compute node, thus we require every element of $(\bar{w}_0^{k-1})_{v_{\max}}$ is less than 1.
 1903 Since $\bar{w}_0^{k-1} = \left(\sum_{j=0}^{k-2} A^j\right) b$, the largest value of $(\bar{w}_0^{k-1})_{v_{\max}}$ satisfies

$$1904 \quad (\bar{w}_0^{k-1})_{\text{largest}} \leq \sum_{j=0}^{k-2} \left(\frac{M-1}{M}\right)^j \times \frac{1}{M} \sum_{i=1}^M \frac{1}{r_i^2} \\ 1905 \quad = M \left(1 - \left(\frac{M-1}{M}\right)^{k-1}\right) * \frac{1}{M} \sum_{i=1}^M \frac{1}{r_i^2} \quad (119)$$

1906 because the maximum value of a_j is $\frac{M-1}{M}$ and the maximum value of b_j is $\frac{1}{M} \sum_{i=1}^M \frac{1}{r_i^2}$.

1907 Thus we require

$$1908 \quad \sum_{i=1}^M \frac{1}{r_i} < \frac{1}{1 - \left(\frac{M-1}{M}\right)^{k-1}}. \quad (120)$$

1909 Since $\left(\frac{M-1}{M}\right)^{k-1} \rightarrow 0$ when $k \rightarrow \infty$, we only require the LHS is less than the lower bound of RHS:

$$1910 \quad \sum_{i=1}^M \frac{1}{r_i} < 1. \quad (121)$$

1911 Therefore we can choose $r_i = M+1$ to make it happen.

1912 Then we can obtain $\beta_{ij}^k > 0$ holds for any support vector x_{ij} and any round k . And the \tilde{w}_i^k simply satisfies
 1913 $X_{S_i} \tilde{w}_i^k = -\ln \beta_i^k$. \square

1944 D.3 LEMMA AND PROOFS IN SECTION 4.4
1945

1946 Here we provide a lemma of Modified Local-GD similar to Lemma 1 of vanilla Local-GD.

1947 **Lemma 11.** *For almost all datasets sampled from a continuous distribution satisfying Assumption 1,
1948 we train the global model w_0 from Modified Local-GD and \bar{w}_0 from Modified PPM. The parameter
1949 is chosen as $\alpha^k = 1 - \frac{1}{k+1}$. With initialization $w_0^0 = \bar{w}_0^0 = 0$, we have $w_0^k \rightarrow \ln\left(\frac{1}{\lambda}\right)\bar{w}_0^k$, and the residual
1950 $\|w_0^k - \ln\left(\frac{1}{\lambda}\right)\bar{w}_0^k\| = O(k \ln \ln \frac{1}{\lambda})$, as $\lambda \rightarrow 0$. It implies that at any round $k = o\left(\frac{\ln(1/\lambda)}{\ln \ln(1/\lambda)}\right)$, w_0^k converges
1951 in direction to \bar{w}_0^k :*

1952
$$\lim_{\lambda \rightarrow 0} \frac{w_0^k}{\|w_0^k\|} = \frac{\bar{w}_0^k}{\|\bar{w}_0^k\|}. \quad (122)$$

1953 *Proof.* With initialization $w_0^0 = \bar{w}_0^0 = 0$, the Modified Local-GD is just a scaling of vanilla Local-GD:

1954
$$w_0^{k+1} = \frac{k}{k+1} \frac{1}{M} \sum_{i=1}^M w_i^{k+1}. \quad (123)$$

1955 Also, the Modified PPM is a scaling of vanilla PPM: $\bar{w}_0^{k+1} = \frac{k}{k+1} \frac{1}{M} \sum_{i=1}^M \bar{w}_i^{k+1}$.1956 When $k \geq 1$, we can know the residual between Modified Local-GD and Modified PPM is

1957
$$\begin{aligned} \|r^k\| &= \left\| w_0^k - \ln\left(\frac{1}{\lambda}\right)\bar{w}_0^k \right\| = \frac{k}{k+1} \frac{1}{M} \left\| \sum_{i=1}^M w_i^k - \ln\left(\frac{1}{\lambda}\right)\bar{w}_i^k \right\| \\ 1958 &\leq \frac{1}{M} \sum_{i=1}^M \left\| w_i^k - \ln\left(\frac{1}{\lambda}\right)\bar{w}_i^k \right\| = \frac{1}{M} \sum_{i=1}^M \|r_i^k\|. \end{aligned} \quad (124)$$

1959 Then we can follow the same process in the proof of Lemma 1 to obtain

1960
$$\|r^k\| \leq \frac{1}{M} \|r_i^k\| = O(k \ln \ln \left(\frac{1}{\lambda}\right)), \quad (125)$$

1961 As a result we have $\lim_{\lambda \rightarrow 0} \frac{w_0^k}{\|w_0^k\|} = \frac{\bar{w}_0^k}{\|\bar{w}_0^k\|}$.1962 \square 1963
1964
1965
1966
1967
1968
1969
1970
1971
1972
1973
1974
1975
1976
1977
1978
1979
1980
1981
1982
1983
1984
1985
1986
1987
1988
1989
1990
1991
1992
1993
1994
1995
1996
1997